Seasonality of isoprenoid emissions from a primary rainforest in central Amazonia

E. G. Alves (1), K. Jardine (2), J. Tota (3), A. Jardine (1), A. M. Yãnez-Serrano(1,4), T. Karl (5), J. Tavares (6), B. Nelson (6), D. Gu (7), T. Stavrakou (8), S. Martin (9), P. Artaxo (10), A. Manzi (1,11), and A. Guenther (7).

(1) Climate and Environment Department, National Institute for Amazonian Research (INPA) and State University of Amazonas (UEA), Av. André Araújo 2936, CEP 69067-375, Manaus-AM, Brazil

(2) Climate Science Department, Earth Science Division, Lawrence Berkeley National Laboratory (LBNL), One Cyclotron Rd, building 64-241, Berkeley, CA 94720, USA.

(3) Institute of Engineering and Geoscience, Federal University of West Para (UFOPA), Rua Vera Paz s/n, CEP 68035-110, Santarem-PA, Brazil.

(4) Biogeochemistry Department, Max Planck Institute for Chemistry, P. O. Box 3060, 55128, Mainz, Germany.

(5) Institute for Meteorology and Geophysics, University of Innsbruck, Innrain 52, A-6020, Innsbruck, Austria.

(6) Ecology Department, National Institute for Amazonian Research (INPA), Av. André Araújo 2936, CEP 69067-375, Manaus-AM, Brazil

(7) Department of Earth System Science, University of California, Irvine, USA.

(8) Belgian Institute for Space Aeronomy, Avenue Circulaire 3, 1180 Uccle, Brussels, Belgium.

(9) School of Engineering and Applied Sciences, Department of Earth and Planetary Sciences, Harvard University, 29 Oxford St ,Cambridge, MA 02138, USA.

(10) Institute of Physics, University of Sao Paulo, Rua Matão, Travessa R, 187 – Cidade Universitária, CEP 05508-900, Sao Paulo-SP, Brazil.

(11) National Institute for Spatial Research, Center of Weather Forecasting and Climate Studies, Rod. Presidente Dutra, km 40, Cachoeira Paulista/SP

Correspondence to: **elianegomes.alves@gmail.com**

Abstract

Tropical rainforests are an important source of isoprenoid and other Volatile Organic Compound (VOC) emissions to the atmosphere. The seasonal variation of these compounds is however still poorly understood. In this study, vertical profiles of mixing ratios of isoprene, total monoterpenes and total sesquiterpenes, were measured within and above the canopy, in a primary rainforest in central Amazonia, using a Proton Transfer Reaction – Mass Spectrometer (PTR-MS). Fluxes of these compounds from the canopy into the atmosphere were estimated from PTR-MS measurements by using an inverse Lagrangian transport model. Measurements were carried out continuously from September 2010 to January 2011, encompassing the dry and wet seasons. Mixing ratios were higher during the dry (isoprene – 2.68±0.9 ppbv, total monoterpenes - 0.67±0.3 ppbv; total sesquiterpenes – 0.09±0.07 ppbv) than the wet season (isoprene – 1.66±0.9 ppbv, total monoterpenes - 0.47±0.2 ppbv; total sesquiterpenes - 0.03±0.02 ppbv) for all compounds. Ambient air temperature and photosynthetically active radiation (PAR) behaved similarly. Daytime isoprene and total monoterpene mixing ratios were highest within the canopy, rather than near the ground or above the canopy. By comparison, daytime total sesquiterpene mixing ratios were highest near the ground. Daytime fluxes varied significantly between seasons for all compounds. The maximums for isoprene (2.53±0.5 μmol m^{-2} h^{-1}) and total monoterpenes (1.77±0.05 μmol m^{-2} h^{-1}) were observed in the late dry season, whereas the maximum for total sesquiterpenes was found during the dry-to-wet transition season (0.77±0.1 μmol m^{-2} h^{-1}). These flux estimates suggest that the canopy is the main source of isoprenoids emitted into the atmosphere for all seasons. However, uncertainties in turbulence parameterization near the ground could affect estimates of fluxes that come from the ground. Leaf phenology seemed to be an important driver of seasonal variation of isoprenoid emissions. Although remote sensing observations of changes in leaf area index were used to estimate leaf phenology, MEGAN 2.1 did not fully capture the behavior of seasonal emissions observed in this study. This could be a result of very local effects on the observed emissions, but also suggest that other parameters need to be better determined in Biogenic Volatile Organic Compound (BVOC) models. Our results support established findings that seasonality of isoprenoids are driven by seasonal changes in light, temperature and leaf phenology. However, they suggest that leaf phenology and its role on isoprenoid

production and emission from tropical plant species needs to be better understood in order to develop mechanistic explanations for seasonal variation in emissions. This also may reduce the uncertainties of model estimates associated with the responses to environmental factors. Therefore, this study strongly encourages long-term measurements of isoprenoid emissions, environmental factors and leaf phenology from leaf to ecosystem scale, with the purpose of improving BVOC model approaches that can characterize seasonality of isoprenoid emissions from tropical rainforests.

Key-words: Isoprene, monoterpenes, sesquiterpenes, leaf phenology, seasonal changes

1. Introduction

Terrestrial vegetation emits high quantities of biogenic volatile organic compounds (BVOCs) to the atmosphere (Guenther et al., 2006, 2012), which are removed by oxidation reactions, deposition of reaction products (Lelieveld et al., 2008) and consumption by surfaces (Gray et al., 2014). Emissions and subsequent transformations in the atmosphere have been widely explored by the scientific community. However, there is still a need for improving our understanding of how BVOC emissions and their reaction products vary seasonally and are involved in atmosphere chemistry, biogeochemical cycling and climate at local, regional and global scales.

Despite a large number of BVOC species that have been identified within plants and in emissions from plants, the largest part of the global biogenic emissions and subsequent effect on atmospheric chemistry are thought to be associated with isoprenoids (Laothawornkitkul et al., 2009). The isoprenoids are an important class of organic compounds that include isoprene (containing five carbon atoms - C_5), monoterpenes (10 carbon atoms - C_{10}), sesquiterpenes (15 carbon atoms - C_{15}) and diterpenes (20 carbon atoms - C_{20}) (Guenther, 2002).

Isoprene, as the building block of the higher order isoprenoids, is the dominant compound in emissions from many landscapes and has the single largest contribution to total global vegetation BVOC emission, with an estimated global annual emission of about

400─600 Tg C (see Table 1 of Arneth et al., 2008). Even though there are more than 1000 monoterpene compounds identified in plants, only a few (less than 12) monoterpenes comprise a large fraction of total monoterpene emissions into the atmosphere (Guenther, 2002). Compounds such as *α*-pinene, *t*-*β*-ocimene, *β*-pinene, limonene, sabinene, myrcene, 3-carene, camphene, *β*-phellandrene and terpinolene dominate monoterpene emissions globally (Guenther et al., 2012). However, at regional scales other monoterpene compounds may also be important (Geron et al., 2000; Jardine et al., 2015). Only a few (e.g., β-caryophyllene) of about 3000 sesquiterpenes and none of the 2000 diterpenes are known to be emitted into the atmosphere in considerable amounts (Guenther, 2002). However, there are many compounds in the atmosphere that are still unknown or unexplored (Goldstein et al., 2007, Park et al., 2013), suggesting that the characterization of sesquiterpene emissions and other trace gases is still an open question.

Although models indicate that tropical rainforests are the main source of isoprenoid emissions to the global atmosphere (Guenther et al., 2012), estimates of global annual emissions of isoprenoid still have large uncertainties (Guenther et al., 2006). One approach to constraining these estimates, specifically for isoprene, is the use of remotely sensed concentrations of BVOC oxidation products in the atmosphere in order to make top-down model estimates (Barkley et al., 2008, 2009, 2013; Stavrakou et al., 2009, 2015). This approach has also suggested seasonal patterns in the emissions of this organic compound (Barkley et al., 2009). In addition, seasonal variations of isoprene emissions in the Amazonian rainforest are suggested based on comparison of some studies with intensive campaigns *in situ* (Table 1). This seasonality may be driven by light and temperature seasonal variation and leaf phenology (Barkley et al., 2009), and seasonal changes in insolation is probably the main driver of leaf phenology (Jones et al., 2014).

Therefore, the objective of this study was to quantify the seasonal variation of mixing ratios and emissions of isoprene, total monoterpenes and total sesquiterpenes in a primary rainforest in central Amazonia and to correlate them to seasonal variations of environmental (temperature and light) and biological (leaf phenology) factors.

2. Material and methods

2.1 Site description

Isoprenoid vertical profiles were investigated at the triangular tower (TT34 tower - 2°35.37′S, 60°06.92′W) on a plateau of the Cuieiras Biological Reserve, a primary rainforest reserve located approximately 60 km northwest of Manaus city, in the central Amazonian Basin, in Amazonas, Brazil (Martin et al., 2010). The vegetation in this area is considered mature *terra firme* rain forest (Pires and Prances, 1985), with a leaf area index of 4.7 (Malhi et al., 2009). The diversity of tree species is above 200 species ha^{-1} (Oliveira et al., 2008). Annual precipitation is about 2500 mm (Fig. 1a), with December to May being the wetter period. Although severe droughts impacted part of the Amazon basin in 2005 and in 2010, those droughts did not affect central Amazonia (Marengo et al., 2008, 2011). However, micrometeorological measurements from 1999 to 2012 showed that from August to September the monthly cumulative precipitation can be less than 100 mm per month (Fig. 1a), characterizing this period as dry season. Average air temperature ranges between 24 °C (in April) and 27 °C (in September) (Fig. 1e). Soil moisture near the surface is slightly reduced (10%) during the dry compared to the wet season (Cuartas et al., 2012).

The period of this study (from September 2, 2010 to January 27, 2011) represents the second half of the dry season (September 2010 - October 2010), the dry-to-wet transition season (November 2010) and the beginning of the wet season (December 2010 - January 2011). The whole period of measurements includes the period of low precipitation and when precipitation is increasing (Fig. 1b), and when photosynthetically active radiation (PAR) (Fig. 1d) and air temperature (Fig. 1f) are at their peaks. As October 2010 had more precipitation only at the end of the month, for this study October 2010 is also considered as dry season. This is supported by the fact that the length and intensity of the dry season varies from year to year (da Rocha et al., 2009).

2.2. Isoprenoid measurements and data analysis

Ambient mixing ratio measurements of isoprene, total monoterpenes and total sesquiterpenes were carried out using a commercial high sensitivity proton-transfer reaction mass spectrometer (PTR-MS, IONICON, Austria). The PTR-MS was operated in standard

conditions with a drift tube voltage of 600 V and drift tube pressure of 2.0 mbar (E/N, 136 Td). During each PTR-MS measurement cycle, the following mass-to-charge ratios (*m*/*z*) were monitored: 21 ($H_3{}^{18}O^+$), 32 ($O_2{}^+$), 37 (H_2O-H_3O^+) with a dwell time of 20 ms each; 69 (isoprene-H^+), 137 (total monoterpenes-H^+) and 205 (total sesquiterpenes-H^+) with a dwell time of 5 s each (Jardine et al., 2011, 2012; Lindinger et al., 1998). The isoprenoid vertical profile was installed with six ambient air inlets at different tower heights (2, 11, 17, 24, 30 and 40 m). Air was sequentially sampled during 10 min at each of the six heights, resulting in one complete profile every hour. Average mixing ratios were calculated for the daytime period (10:00 – 16:00, LT) and for the nighttime period (22:00 – 04:00, LT). Calibration slope (m, ppbv/normalized counts per second (PTR-MS signal)) for isoprene, total monoterpenes, and total sesquiterpenes were obtained twice in the field using the dynamic solution injection technique (Jardine et al., 2010). Solutions of isoprene, α-pinene, and β-caryophyllene standards (> 95% purity, Merk) in 100 mL of cyclohexane were injected into the mixing vial at 0.5, 1.0, 2.0, and 3.0 μL min^{-1} (30 min each flow rate) with a constant dilution flow of 1.0 slpm ultra high purity nitrogen passing through. The linearity of calibrations was significant, being r^2 of 0.92-0.97 for isoprene, r^2 of 0.98-0.99 for α-pinene, and r^2 of 0.90-098 for β-caryophyllene. Sample air isoprenoid mixing ratios were calculated by multiplying the calibration slope by normalized counts per second (PTR-MS signal) (average of two calibration slopes). Calibration slopes obtained on October 2010 were within 10 % relative to those from the calibration carried out in September 2010 (isoprene 7.2 %, α-pinene – 8.2%, and β-caryophyllene – 2.5%). For 4-7 days before each isoprenoid profile measurement period, ultra high purity nitrogen was run into the inlet of the PTR-MS for 2 h in order to obtain the background signals. The limit of detection for isoprene was 0.14 ppbv, 0.15 ppbv for total monoterpenes and 0.1 ppbv for total sesquiterpenes. More details about calibration and experimental design can be obtained in Jardine et al. (2011) and Jardine et al. (2012), in which a subset of these data are already described. While the previous study considered a subset of this data and time period (Jardine et al., 2011, 2012), this study examines the whole dataset and focuses on seasonality of mixing ratios and fluxes. Also, this is the first study in central Amazonia that correlates long-term measurements of isoprenoids, light and temperature, and leaf phenology.

179

180 **2.3 Isoprenoid gradient flux, and modeled flux estimates - Model of Emissions of**
181 **Gases and Aerosols from Nature (MEGAN 2.1)**

182 Fluxes of isoprene, total monoterpenes and total sesquiterpenes - for dry, dry-to-wet
183 transition and wet seasons - were estimated using the average daytime (10:00-14:00, LT)
184 concentration vertical profile throughout the canopy and applying an inverse Lagrangian
185 transport model (ILT) (Raupach, 1989; Nemitz et al., 2000; Karl et al., 2004; Karl et al.,
186 2009). The source/sink distributions throughout the canopy were computed according to
187 Eq. (1):

188 $$\vec{C} - C_{Ref} = \overleftrightarrow{D} . \vec{S} \quad (1)$$

189 where $\vec{C}$ is the concentration (g m^{-3}) vector for the 6 levels, C_{Ref} is the concentration (g m^{-3})
190 at reference height (40 m), $\overleftrightarrow{D}$ (m) is a dispersion matrix, and $\vec{S}$ (mg m^{-2} h^{-1}layer^{-1}) is the
191 resulting source/sink vector. $\overleftrightarrow{D}$ is expressed as a function of Lagrangian timescale and
192 profiles of the standard deviation of the vertical wind speed (σ_w), which was normalized to
193 friction velocity (u*). Integration over all source and sink terms ($\vec{S}$) yielded the canopy
194 scale isoprenoid flux (mg m^{-2} h^{-1}). To parameterize $\overleftrightarrow{D}$, we use the Lagrangian timescale (Tl)
195 parameterized according to Raupach (1989) and the vertical profile of the standard
196 deviation of the vertical wind speed scaled to measured friction velocity. The normalized
197 turbulence profile was taken from turbulence measurements inside and above the canopy at
198 this site recorded as part of AMAZE-08 (Amazonian Aerosol Characterization Experiment
199 2008) (Karl et al., 2009). The friction velocity was averaged for each season using daytime
200 data (10:00-14:00, LT) measured at a tower (K34 tower - 2° 36' 32.67" S, 60° 12' 33.48"
201 W) that was 2 km away from the tower where isoprenoid profiles were measured (TT34
202 tower). The calculation of $\overleftrightarrow{D}$ was based on the far- and near-field approach described by
203 Raupach (1989). As some model inputs (i.e., σ_w/ u*) were obtained during the wet season
204 at the TT34 tower in 2008 (Karl et al., 2009), changes in canopy structure between the two
205 studies could potentially affect the results of this study. However, previous work carried out
206 at the K34 tower showed that u* along with other averaged turbulence data have quite
207 similar daytime values in both wet and dry seasons (Ahlm et al., 2010; Araujo et al., 2002).

Once fluxes from the isoprenoid vertical profiles were obtained by the ILT, they were compared with the isoprenoid fluxes estimated by the Model of Emissions of Gases and Aerosols from Nature (MEGAN 2.1). Isoprenoid emissions estimated by MEGAN 2.1 are based on a simple mechanistic model that takes into account the main processes driving variations in emissions (Guenther et al., 2012). As described by Guenther et al., (2012), the activity factor for isoprene, monoterpenes and sesquiterpenes (γ_i) considers the emission response to light (γ_P), temperature (γ_T), leaf age (γ_A), soil moisture (γ_{SM}), leaf area index (LAI) and CO_2 inhibition (γ_{CO2}) according to Eq. (2):

$$\gamma_i = C_{CE}\, LAI\, \gamma_P \gamma_T \gamma_A \gamma_{SM} \gamma_{CO_2} \quad (2)$$

where C_{CE} is the canopy environment coefficient. For the present study, the canopy environment model of Guenther et al. (2006) was used. It has a C_{CE} of 0.57. MEGAN 2.1 was run with variation in light and temperature and LAI. Leaf age of the foliage was estimated by the model based on changes in LAI. Soil moisture and CO_2 inhibition activity factors were assigned a value γ_{SM} = 1 and γ_{CO2} = 1, respectively, which assumes no variation in these parameters. More details about the model settings can be obtained in Guenther et al. (2012).

Photosynthetic photon flux density (PPFD) and air temperature for all model runs were obtained from the K34 tower measurement time series (Program of Large Scale Biosphere-Atmosphere – LBA). LAI inputs were obtained by satellite observations from NASA MODIS during August 2010 to January 2011. The level-4 LAI product is composited every 8 days at 1-km resolution on a sinusoidal grid (MODIS-NASA, 2015).

2.4 Uncertainties associated with the ILT and BVOC emission modeling

The main source of errors for applying the ILT is related to the parameterization of two combined effects: (1) vertical diffusion coefficient which is based on measured σ(w)/u* profiles, and (2) Langrangian dispersion time scale (Tl). Moreover, some uncertainties may be due to systematic error sources with respect to (3) chemical losses, and (4) the number of source layers. The entire parameterization of combined effect (1) and (2) was tested using data from an earlier study (Karl et al., 2009, Karl et al., 2010), where a comparison with eddy covariance measurements was available. Taking the above conservative error assessment, the combined (effect 1 and 2) uncertainty is +/- 30%.

To account for chemistry (effect 3) we used a simple modification of the diffusion coefficient based on Hamba (1993), relying on the fact that the chemical loss will mainly influence the far field of the parameterization. Based on estimated OH and measured O_3 densities (Karl et al. 2009, Karl et al., 2010) calculated VOC fluxes were corrected accordingly. Due to low OH and O_3 densities in the canopy (<5 x 10^5 molecules cm^{-3} for OH and <10 ppbv for O_3) the chemical lifetime for isoprene and monoterpenes is considered large compared to the mixing timescale, leading to a chemistry correction on the order of <5% for isoprene and monoterpenes. This systematic error is included, but relies on an estimation of OH for isoprene. The overall uncertainty for isoprene is calculated as 0.3 – 4 % by varying in-canopy OH densities between 5 x 10^5 and 5 x 10^6 molecules cm^{-3}. It is noted that an in-canopy OH density of 5 x 10^6 molecules cm^{-3} is extremely unrealistic in such a dense canopy and only serves as a very conservative upper limit. Those assumptions were also considered for sesquiterpene flux estimates. However, a sensitivity test was carried out to show if the increasing ozone concentrations during the dry season could effectively affect sesquiterpene lifetime and then sesquiterpene flux estimates. For this test, sesquiterpene lifetime was changed in the ILT model using a range from 2 min to 8 hours (upper limit used for isoprene and monoterpene flux estimates). The lower limit (2 min) is based on the lifetime calculated for β-caryophyllene when it is exposed to 24-h average of 7 x 10^{11} molecules cm^{-3} of ozone (~30 ppb) (Atkinson and Arey, 2003). If all sesquiterpenes that occur in this site have similar reactivity with ozone as β-caryophyllene, the overall uncertainty for sesquiterpene flux estimates is calculated as up to 20% by varying sesquiterpene lifetime from 8 h to 2 min. It is noted that when considering a lifetime range from 8h to 10 min, the uncertainty for sesquiterpene flux estimates is calculated as up to 4%. The 20 % of uncertainty may be important only during the dry season, when ozone mixing ratios can eventually reach 30 ppbv above canopy (40 m) around noontime.

We have also investigated the effect of (4) - the number of source layers. If the number of selected source layers is too small, systematic errors of the calculated integrated fluxes arise. We have investigated this effect and found that in the present case, six source layers are sufficient to capture >90% of the flux. In the present setup, the ILT model does not converge for more than nine layers and the numerical solution becomes unstable. If the

ILT model would be initiated to only calculate two source layers, the integrated flux would be underestimated significantly (e.g. by up 50%). With 6 source layers we estimate a systematic error of <10% due to this effect. The combined effect of the systematic errors (3) and (4) is estimated to be 5-6%.

With respect to uncertainties in model estimates, one of the first quantitative estimates of biogenic VOC emissions (Lamb et al., 1987) included an estimate of uncertainty of 210% based on the propagation of uncertainties in emission factors, emission algorithms, amount of biomass, and land use distributions. This "factor of three" uncertainty has continued to be used as a rough assessment of the uncertainty of biogenic VOC emission model estimates applied on regional scales. A more recent study (Hanna et al., 2005) attempted a comprehensive assessment of each model component and concluded that the 95% confidence range on the calculated uncertainty in isoprene emission was about one order of magnitude while the calculated uncertainty for monoterpenes and other VOC was only ± 20%. Guenther (2013) suggests that the Hanna et al. (2005) study assigns isoprene a higher uncertainty only because more is known about isoprene, and so there are more parameters, and that the lack of observations for quantifying the uncertainties associated with individual model parameters limits the usefulness of this uncertainty estimation approach and instead recommends evaluations that consider the results of model comparisons with canopy scale observations. These studies indicate that models tend to agree with observations within ~30% for canopy scale studies with site specific parameters (Lamb et al., 1996) or for regional scale estimates with known land cover (Misztal et al., 2014) and differ by as much as a factor of two or more for other regional scale studies (Muller et al., 2008; Warneke et al., 2010).

2.5 Canopy light penetration and leaf phenology

The standard canopy environment model of MEGAN 2.1 was used to model light penetration into the canopy (Guenther et al., 2006). Model inputs included the above-canopy PAR measured (every 30 min) at 50 m on the K34 tower for the whole period of isoprenoid measurements as well as the estimated surface area density of the canopy (m^2 m^{-3}), with measurements carried out in March 2004 using a Light Detection and Ranging

sensor (LIDAR) in a transect on the same plateau area of this study (Parker and Fitzjarrald, 2004).

The light penetration was modeled for five canopy layers distributed from the canopy top to the ground surface. The thickness of each of the five layers was determined based on the canopy surface area density estimated for every 50 cm from the ground surface to the top canopy (Parker and Fitzjarrald, 2004). The layers were distributed according to a Gaussian curve fit to the canopy surface area densities (from 0.5 m to 48 m). Light absorption was calculated as the difference in the model estimate of downward light at the top and bottom canopy levels. This light absorption corresponded to light that passed through the canopy vertically. Reflectance and scattering were not considered.

Leaf phenology was estimated based on the observation of leaf flushing events of the upper crown surfaces of 63 living trees around the K34 tower (~ 2 km far of TT34 tower). For this approach, it is assumed that the leaf phenology of the upper crown surfaces of trees around both towers is similar. For the monitoring, a system of data acquisition and storage, based on a Stardot (model Netcam XL 3MP) camera with a 1024 x 768 resolution CMOS sensor, was installed at K34 tower, at 15-20 m above the canopy. The camera viewing angle was south azimuth, perpendicular to the solar transit, centered on 32º of depression and pointing out to an area of plateau. Images were logged every 15 s to a passively cooled FitPC2i with heat-tolerant SSD drive. The whole system of data acquisition automatically rebooted after power outages. The images obtained by the camera covered approximately 66º horizontally and 57º vertically, fitting the forest canopy without including any area of sky in the image. The most distant trees in the image were located 150 m from the camera. The framework was fixed by monitoring the same 63 treetops over four months of observation (October 2010 – January 2011). The analysis of images was based on the number of treetops that showed leaf flushing within one month. For this, one image was selected at every six days, and then grouped for each month of this study.

2.6 Satellite-derived isoprene emission estimates

Top-down isoprene emission estimates over the 0.5 degree region around TT34 tower were obtained by using a grid-based source inversion scheme (Stavrakou et al., 2009) constrained by formaldehyde (HCHO) columns. HCHO is an intermediate product of the

isoprene degradation process (e.g. Stavrakou et al., 2014). It is measured by UV-visible sensors, such as on the Global Ozone Monitoring Experiment (GOME-2)/MetOp satellite launched in 2006. The source inversion was performed using the global chemistry-transport model IMAGESv2 (Intermediate Model of Annual and Global Evolution of Species) run at a resolution of 2º × 2.5º and 40 vertical levels from the surface to the lower stratosphere (Stavrakou et al., 2014, 2015). The priori isoprene emission inventory is taken from MEGAN-MOHYCAN-v2 (Stavrakou et al., 2014, http://tropo.aeronomie.be/models/isoprene.htm), and includes updates regarding isoprene emission rates from Asian tropical forests. IMAGESv2 uses HCHO columns retrieved from GOME-2 sensor as top-down constraints and estimates the posterior biogenic isoprene emission on the global scale. Note that given the early morning (9:30) overpass time of the GOME-2 measurement, and the mostly delayed production of formaldehyde from isoprene oxidation, the top-down emission estimate is dependent on the ability of MEGAN to simulate the diurnal shape of isoprene emission and on the parameterization of chemical and physical processes affecting isoprene and its degradation products in IMAGESv2. For this study, we use daily (24 hours) mean satellite-derived isoprene emissions derived from January 2010 to January 2011. More details can be found in Stavrakou et al. (2009, 2014, 2015) and Bauwens et al. (2013).

3. Results and Discussion

3.1 Diurnal variation of isoprenoid mixing ratios

Vertical profiles of isoprenoids were analyzed for daytime and nighttime for all the seasons considered in this study. Isoprene (Fig. 2 a, b, c) and total monoterpenes (Fig. 2 d, e, f) had higher mixing ratios during daytime (10:00-16:00, LT) than during nighttime (22:00-04:00, LT) for all seasons, supporting the findings that emissions of isoprene (Alves et al., 2014; Harley et al., 2004) and monoterpenes (Bracho-Nunez et al., 2013; Kuhn et al., 2002, 2004a; Jardine et al., 2015) from Amazonian plant species, at least at this site, are primarily light-dependent and stimulated by increasing temperature.

During daytime, isoprene had a maximum mixing ratio within the canopy. By comparison, at nighttime maximum values occurred above the canopy, and the vertical

profiles were similar to those of nighttime air temperature (Fig. 2 j, k, l). As isoprene is not emitted at night, this maximum nighttime abundance of isoprene above the canopy may be due to the daytime residual layer concentrations. In addition, isoprene lifetime increases during nighttime owing to the decrease of OH (hydroxyl radical) concentrations in the dark (Goldan et al., 1995) in light of the low concentrations of nitrogen oxides (NO_x) in Amazonia (≤ 3 ppb above the canopy during nighttime in the dry-to-wet transition season) (Andreae et al., 2002). Similar results found at another site in central Amazonia suggested that low isoprene concentrations near the ground after sunset could be due to deposition onto and consumption by surfaces (Yáñez-Serrano et al., 2015). Isoprene up-take in the soil has been suggested previously in central Amazonia (Silva, 2010), possibly because of isoprene microbial consumption (Cleveland and Yavitt, 1997; Gray et al., 2014). As with isoprene, higher mixing ratios of total monoterpenes were observed during daytime, indicating that they are light-dependent, which agrees with the evidence of recent photosynthetic origin of monoterpenes (Jardine et al., 2015; Loreto et al., 1996).

The vertical profile of total sesquiterpene mixing ratios differed from that of isoprene and total monoterpenes for all seasons. Total sesquiterpenes had higher mixing ratios near the ground and at the sub-canopy level (17 m) than above the canopy (Fig. 2 g, h, i) ($P < 0.05$). Daytime and nighttime vertical profiles had similar shape, but total sesquiterpene mixing ratios were higher during the nighttime. Even though sesquiterpene emissions for some plant species are both light- and temperature-dependent (Duhl et al., 2008), results reported here indicate that sesquiterpene emissions are not strongly light-dependent in this site, suggesting that their daily variation is driven primarily by temperature. Since some studies have shown that sesquiterpenes are found in the essential oil stored in Amazonian forest trees (e.g. Lima et al., 2005), emissions from these storage structures would not be expected to be light-dependent. In contrast, the monoterpenes, while also present in Amazonian tree essential oil (e.g. Fidelis et al., 2012; Lima et al., 2005), appear to be dominated by emissions that occur with no storage (e.g. Loreto et al., 1996; Jardine et al., 2015), similar to isoprene emission processes. Another reason for the higher total sesquiterpene mixing ratios at nighttime might be because of the reduction of oxidative reactions owing to the decrease of OH concentrations in the dark (Goldan et al., 1995) and low concentrations of nitrogen oxides (NO_x) (Andreae et al., 2002), ozone, and

392 nitrate (NO_3) in Amazonia (Martin et al., 2010). In addition, ozonolysis of sesquiterpenes
393 during daytime can reduce ambient sesquiterpene concentrations, as previously reported for
394 a subset of these data (Jardine et al., 2011). With daytime ozone mixing ratios up to 40
395 ppbv (40 m) during the dry season, sesquiterpene lifetime with respect to ozonolysis above
396 the canopy (40 m) can be 2 min during the daytime and 5 min during the nighttime (Jardine
397 et al., 2011). Additionally, sesquiterpene concentrations can build up near the surface,
398 because during nighttime the storage in the forest dominates (80-90%) and is significantly
399 larger than the turbulent flux (Karl et al., 2004).

400

401 **3.2 Seasonal variation on isoprenoid mixing ratios and emissions**

402 Vertical profiles of isoprene had higher mean mixing ratios in the dry season,
403 followed by the dry-to-wet transition season and wet season (top panel of Fig. 3 a). The
404 reduction of isoprene mixing ratios from the dry season to dry-to-wet transition season was
405 up to 20% and from dry season to wet season was up to 65%. During the dry season, the
406 higher mixing ratios and emissions of isoprene have been attributed to the higher insolation
407 and higher temperatures compared to the wet season and, for this reason, higher isoprene
408 concentrations at the top of the canopy are expected. Nevertheless, in contrast to the
409 observations of Yañez-Serrano et al. (2015), who reported maximum daytime mixing ratios
410 of isoprene at the top of the canopy for both dry and wet seasons, this study showed the
411 highest isoprene mixing ratios inside the canopy (11 m) during the dry season, with this
412 maximum moving to the upper canopy during the dry-to-wet transition season (24 m).
413 Isoprene emissions inferred from concentration vertical profiles were estimated to
414 be highest in the sub-canopy (16 m) during the dry season and in the upper canopy (28 m)
415 during the dry-to-wet transition season and the wet season (Fig. 4 a). Even though there
416 were differences in which layer was the highest emitter of isoprene within the canopy,
417 mean isoprene emissions into the atmosphere were about the same for the dry season and
418 the dry-to-wet transition season (1.37 ± 0.7 mg m^{-2} $h^{-1}$and 1.41 ± 0.1 mg m^{-2} h^{-1},
419 respectively). Both of these seasons had higher isoprene emissions than during the wet
420 season (0.52 ± 0.1 mg m^{-2} h^{-1}) (Fig. 4 b).

421 The maximum absorption of PPFD by canopy, calculated based on PPFD
422 penetration profile modeled by the standard MEGAN 2.1 canopy environment model,
423 occurred right above the maximum of estimated surface area density of the canopy, with
424 the absorption of PPFD being higher during the dry season, followed by the wet season and
425 the dry-to-wet transition season (Fig. 3 b). This maximum PPFD absorption at the upper
426 canopy agreed with the maximum of isoprene mixing ratios (top panel of Fig. 3 a) and
427 emissions (Fig. 4 a) during the dry-to-wet transition season. It differed, however, when
428 compared to peaks of isoprene mixing ratios and emissions during the dry season and the
429 wet season.

430 One reason for this difference could be the isoprene oxidation in the atmosphere and
431 within plant, especially at the top of the canopy. During the dry season the ratio of methyl
432 vinyl ketone + methacrolein + hydroperoxides (MVK+MAC+ISOPOOH) (Liu et al., 2013)
433 to isoprene was higher compared to the dry-to-wet transition and the wet season (data not
434 shown). This higher ratio may indicate an increased oxidative capacity of the atmosphere
435 during the dry season. Moreover, a small source of MVK+MAC+ISOPOOH was observed
436 at the top of the canopy (Jardine et al., 2012). Under conditions of high abiotic stress, as
437 can occur in the dry season, elevated isoprene oxidation rates in plants can be observed and
438 isoprene oxidation products might be directly emitted by plants (Jardine et al., 2012).

439 Another important factor might be leaf phenology and/or leaf demography.
440 Different tree species have different isoprene emissions rates, and these rates depend upon
441 the leaf ontogenetic stage. Isoprene emitters can flush at different canopy levels seasonally,
442 and changes in within-canopy isoprene vertical profiles would be expected as a result.
443 Moreover, as more leaf flushing was observed at the upper canopy during the wet-to-dry
444 transition and early dry season, this caused leaves in the age group of 3-8 months to reach
445 the highest abundance in late dry season and early wet season (Nelson *et al.*, 2014). The
446 period with the high abundance of leaves in this age group is coincident with the period
447 when gross ecosystem productivity and landscape-scale photosynthetic capacity is most
448 efficient (Restrepo-Coupe et al., 2013). Here, results show maximum isoprene emission at
449 the upper canopy during the dry-to-wet transition season (Fig. 4 a), which is coincident
450 with the period of high abundance of healthy efficient leaves at the canopy top (Nelson et
451 al., 2014) and also coincident with the maximum isoprene emission shown in young mature

leaves in the dry-to-wet transition season (Alves et al., 2014). Similarly, higher isoprene emissions during the late dry season have also been related to the increase of active biomass in southern Amazonia (Kesselmeier et al., 2002; Kuhn et al., 2004a, 2004b).

Although the isoprene mixing ratios reported here are within the range of previously reported values in central Amazonia for the dry season and the dry-to-wet transition season (Greenberg and Zimmerman, 1984; Rasmussen and Khalil, 1988; Zimmerman et al., 1988) and for the wet season (Yáñez-Serrano et al., 2015), these results are the lowest observed fluxes of isoprene to atmosphere reported for the Amazonia. However, this could be due to the particular location of the site of this study, such as the relatively open canopy, caused by the proximity to a dirt road, and perhaps the site has a relatively low fraction of isoprene emitting species. Isoprene fluxes measured previously at the same tower site during the wet season were similar (Karl et al., 2009).

Total monoterpenes also showed a strong seasonal variation with maximum mixing ratios during the dry-to-wet season, followed by the dry season and the wet season (middle panel of Fig. 3 a). Taking mixing ratios of the dry-to-wet transition season as a reference, total monoterpene mixing ratios showed an increase of up to 20% from the dry season to the dry-to-wet transition season, and a decrease of up to 50% from the dry-to-wet transition season to the wet season. Although total monoterpene mixing ratios were somewhat higher in the dry-to-wet transition season than during the dry season, total monoterpene fluxes inferred by the vertical profiles were slightly higher during the dry season (1.47 ± 0.06 mg m^{-2} h^{-1}) compared to the dry-to-wet season (1.29 ± 0.2 mg m^{-2} h^{-1}) (Fig. 4 e), indicating that the production is higher in the dry season and losses are also higher, leading to lower mixing ratios. In comparison, emissions from these two seasons were considerably higher than during the wet season (0.36 ± 0.05 mg m^{-2} h^{-1}) (Fig. 4 e). This again indicates that higher insolation and air temperature during the dry season and dry-to-wet transition season compared to the wet season increased the atmospheric concentrations of monoterpenes and, considering the enhanced ozone mixing ratios during the dry season, this may influence the seasonal pattern in monoterpene ozonolysis loss rates (Jardine et al., 2015). These results agree with branch level measurements that showed higher monoterpene emissions during the dry-to-wet transition season compared to the wet-to-dry transition season (Kuhn et al., 2004a). However, results reported here differ from those presented for the southern

Amazonia, where monoterpene mixing ratios were higher during the wet season than during the dry season (Kesselmeier et al., 2002). Although only a few studies have been carried out with the objective of investigating monoterpene seasonal variations, factors other than light and temperature might influence monoterpene emissions from vegetation, including the oxidative capacity of the atmosphere and leaf phenology (Kesselmeier et al., 2002; Kuhn et al., 2004a).

Total monoterpene mixing ratios and fluxes, during the dry season and the dry-to-wet transition season, were similar to values reported for other sites in central Amazonia (Karl et al., 2007; Yáñez-Serrano et al., 2015). However, the monoterpene comparison of reported studies is a difficult endeavor given that some techniques measured total monoterpenes and others measured some specific monoterpene compounds, and also because monoterpene fragmentation during measurements (PTR-MS) could affect the absolute values of these compounds. Therefore, further efforts are needed in order to characterize the seasonal abundance and the seasonal species-specific composition of monoterpenes in the Amazonia.

Average vertical profiles of total sesquiterpene mixing ratios were higher in the dry-to-wet transition season, followed by the dry season and the wet season (bottom panel of Fig. 3a). Taking mixing ratios of the dry-to-wet transition season as a reference, total sesquiterpene mixing ratios increased up to 30% from the dry season to the dry-to-wet transition season and decreased by up to 55% from the dry-to-wet transition season to the wet season. During the dry season and the dry-to-wet transition season, the maximum total sesquiterpene mixing ratios were observed near the ground. During the wet season, the maximum mixing ratio was at 17 m (sub-canopy). According to Jardine et al. (2011), during the daytime many sesquiterpenes (46%–61% by mass) are rapidly oxidized by ozone as they undergo within-canopy ozonolysis and contribute to the scarcity of total sesquiterpenes above and near the top of the canopy. Considering that higher insolation and also higher ozone concentrations were observed during the dry season (ozone daily average of ~ 23 ppbv and ~ 10 ppbv at 40 m in the dry and wet seasons, respectively), an important fraction of the sesquiterpenes emitted by vegetation could be rapidly oxidized by ozone, leading to significantly lower mixing ratios of total sesquiterpene during the dry season

513 (Jardine et al., 2011), which creates a need to account for sesquiterpene oxidation within
514 the canopy when calculating emission rates.

515 Another potential reason for higher mixing ratios of total sesquiterpenes near the
516 ground is that emission could come from surface sources including litter, roots and soil
517 microbes and fungi. Silva (2010) presented surface BVOC emissions at this site, and the
518 results suggested that the litter decomposition could be an important source of
519 sesquiterpenes to the atmosphere. Litter production is higher during the dry than during the
520 wet season (Luizão et al., 1989), which could lead to higher amounts of litter at the end of
521 the dry season. Rain starting to increase in the dry-to-wet transition could contribute to
522 more decomposition of the litter storage, which can potentially increase sesquiterpene
523 emissions during the processes of decomposition of dead organic matter. Although the
524 ecological functional role of these sesquiterpenes is not known, abiotic emissions from the
525 litter have a specific signature that can be similar to the concentration profile in the green
526 leaf content (Austin et al., 2014) and in sufficient concentration BVOCs can have the
527 capacity of attracting and repelling soil organisms to a specific location (Austin et al.,
528 2014). Therefore, higher sesquiterpene emissions from the litter could be a signal to the
529 fauna related to the decomposition process and represent an important step of the
530 biogeochemical cycling.

531 In contrast to the mixing ratios, the source-sink distribution analysis made from the
532 vertical profiles of total sesquiterpenes indicated that the main source of these compounds
533 is the canopy (24 m) (Fig. 4 g), and the integration of sources and sinks showed that the
534 highest total sesquiterpene emission rates going into the atmosphere was during the dry-to-
535 wet transition season (0.77 ± 0.1 mg m^{-2} h^{-1}), followed by the dry season (0.38 ± 0.2 mg m^{-2}
536 h^{-1}), and the wet season (0.34 ± 0.2 mg m^{-2} h^{-1}) (Fig. 4 h). However, although Nemitz et al.
537 (2000) have suggested that limitations on the σ_w/u^* parameterization close to the ground do
538 not affect the net flux above the canopy, here we strongly suggest future studies focus on
539 better characterizing the turbulence and oxidation processes at this site, in order to verify
540 the source-sink distribution of sesquiterpenes within the canopy and the emissions from the
541 canopy to atmosphere. This should include speciated sesquiterpene measurements in order
542 to account for their specific reactivity with ozone and other oxidants.

543 Relative emissions can be calculated as emissions normalized to standard conditions
544 of above-canopy PAR of 1500 μmol m^{-2} s^{-1} and temperature of 30 °C. Based only on light,
545 temperature and LAI variation, relative emissions estimated by MEGAN 2.1 were
546 maximum during the dry season for isoprene, α-pinene, and β-caryophyllene (Fig. 4 c, f, i),
547 when the highest light and temperature were observed. This prediction differs from the ILT
548 flux estimates (Fig. 4 b, e, h), which showed similar emissions between the dry and the dry-
549 to-wet season for isoprene and total monoterpenes and maximum emission during the dry-
550 to-wet season for total sesquiterpenes. The overall uncertainties related to ILT flux was
551 calculated as ± 36% and MEGAN estimates are considered to be in agreement with
552 observations when they are within ~30%. However, more observation studies are needed in
553 order to evaluate the degree of observation-modeling agreement and to improve model
554 approaches, especially for total monoterpenes and total sesquiterpenes, which could present
555 larger uncertainties due to the lack of information about atmospheric concentrations and
556 reactivity of monoterpene and sesquiterpene chemical species in Amazonia.

557 To compare the seasonal variation of isoprenoid emissions with changes in
558 environmental (light and temperature) and biological (LAI) factors in more detail, monthly
559 fluxes of isoprenoids were compared to PAR at 51 m, air temperature at 51 m, and LAI
560 (satellite observations - MODIS) (Fig. 5). The highest fluxes of isoprene and total
561 monoterpene were observed when PAR was at its highest (October 2010) (Fig. 5 b, c), and
562 when there is high abundance of healthy efficient leaves (Nelson et al., 2014). The
563 similarity in the behavior of isoprene and monoterpene emissions is supported by the
564 evidence of the photosynthetic origin of monoterpenes (Jardine et al., 2015; Loreto et al.,
565 1996). Interestingly, in September 2010 total monoterpene emissions were higher than
566 isoprene emissions. This could be related to the higher source of monoterpenes in the upper
567 canopy compared to isoprene during this month. When there are more young leaves at the
568 upper canopy during the first half of the dry season (Nelson et al., 2014), high emissions of
569 monoterpenes can be expected. Total sesquiterpene fluxes tracked neither PAR nor air
570 temperature, having the highest emission when PAR and air temperature were decreasing
571 (November 2010) (Fig. 5 d).

572 Predictions from MEGAN 2.1 again differed from measured emissions (Fig. 5 b, c,
573 d), showing a reduction in emissions from September 2010 to January 2011. Major

574 quantitative differences between ILT and MEGAN estimates can be shown for isoprene in
575 September, when ILT estimates represented only 4 % of the MEGAN estimates; for total
576 monoterpenes in December, when ILT estimates accounted for 14 % of the MEGAN
577 estimates; and for total sesquiterpenes in November, when ILT estimates were 232% of the
578 MEGAN estimates". These differences may be related to local effects, especially leaf
579 phenology and changes in the atmospheric oxidative capacity over the seasons. In order to
580 evaluate the potential effect of leaf phenology on emissions, leaf flushing, PAR, isoprene
581 and total monoterpenes at canopy scale were compared in Fig. 6. They closely tracked each
582 other during the 4 months of measurements. For the period of this study, the analysis of
583 canopy images for every six days from October 2010 to January 2011 showed a decrease in
584 leaf flushing from the end of the dry season to the wet season, which was similar to the
585 decrease of isoprene and total monoterpene emissions and PAR. Results from 28 months
586 (October 2010-January 2013) of canopy imaging have shown that the highest number of
587 treetops with leaf flushing occurred during the wet-to-dry transition season (June-July),
588 accounting for 35-50 % of treetops with leaf flushing, followed by a subsequent decrease
589 until the end of the wet season (Tavares, 2013) (Fig. 6). Correspondingly, the results of the
590 present study suggest that lowest emissions might be expected in the June-July time period.
591 These results agree with those presented by Barkley et al. (2009) using remote sensing,
592 suggesting that seasonal changes in isoprene emissions may be strongly affected by leaf
593 phenology in the Amazonia.

594 In order to verify if the seasonal trend of the isoprene emissions observed in this
595 study can also be observed in a 0.5° grid cell around TT34 tower, isoprene emissions
596 estimated based on tower vertical profile concentrations are compared with estimates
597 constrained by satellite measurements of HCHO in Fig. 7. The top-down estimates have a
598 seasonal cycle that is similar to the bottom-up approach. Compared to the dry season,
599 fluxes decrease by 40% during the wet and the wet-to-dry transition season from April to
600 July (Stavrakou et al., 2015), in qualitative agreement with the conclusions drawn in
601 Barkley et al. (2009). The inferred dry season isoprene flux is about twice that of the wet-
602 to-dry season. It peaks in September and gradually drops from October to January (Fig. 7),
603 as a result of decreasing temperature and solar radiation, affecting the oxidation of isoprene
604 leading to HCHO formation. The ground-based estimates exhibit a much stronger month-

605 to-month variation, with flux estimates of 5 times higher in October compared to
606 September and December. The small increase of the flux between December and January is
607 not observed by the satellite observations. Despite these differences, partly due to reduced
608 representativeness when comparing local measurements with flux estimates from a 0.5°
609 grid cell, this comparison shows that both large (satellite) and small (ground-based) scales
610 agree that there are enhanced isoprene emissions during the dry season followed by a
611 reduction towards the wet season.

612 The results reported here are associated with a small footprint area. This together
613 with the huge biodiversity of tropical rainforests makes it impossible to generalize these
614 results to the regional scale. Moreover, although some previous reports have suggested
615 significant seasonal variations of BVOCs based on *in situ* measurements in different sub-
616 regions of Amazonia, when those investigations (summarized in Table 1) and this study
617 were compared, high variability is apparent among values of mixing ratios and fluxes. This
618 variability could be due to: (1) different methodologies, (2) sampling in different seasons,
619 (3) sampling in different regions (e.g., south, north, west, eastern Amazonia), (4) sampling
620 in different ecotones of the same region, (5) different statistical analyses, and (6) perhaps
621 due to small data sets that are not statistically significant to characterize emissions of a
622 specific site.

623

624 **3.3 Comparison with model predictions of seasonal isoprenoid emissions in Amazonia**

625 Although the canopy scale isoprenoid emission measurements presented here
626 differed from those modeled by MEGAN 2.1 (Figs. 4 and 5), which assume that variations
627 are driven primarily by light, temperature and leaf area, in terms of seasonal variation,
628 MEGAN 2.1 estimates of isoprene emission agreed fairly well with the satellite-derived
629 isoprene emission, which suggests that other factors at this site could influence isoprene
630 emissions locally. As already mentioned, leaf phenology may cause important effects on
631 local emissions. As MEGAN 2.1 was driven with local variations in PAR and air
632 temperature, and with regional variations of LAI (satellite observations at 1-kilometer
633 resolution), this regional variation in LAI may not represent the local effect of LAI
634 variation on local emissions, since vegetation in Amazonia is phenologically distinct due to
635 the huge biodiversity of this ecosystem (Silva et al., 2013). Furthermore, as the canopy

636 structure might vary seasonally due to leaf phenology/demography, the pattern of light
637 penetration/absorption and then leaf temperature may change as well; thus, this, together
638 with the differences in emissions among species and among leaf ontogenetic stages, could
639 have an important impact on seasonal changes of local emissions.

640 Besides the effects of light, temperature and leaf phenology/demography, some
641 efforts have been made to include effects of CO_2 variation (Arneth et al., 2007; Guenther et
642 al., 2012) as well as the link between photosynthesis and emission (Grote et al., 2014;
643 Morfopoulos et al., 2013, 2014; Unger et al., 2013) into isoprene emission models at
644 regional and global scales. However, the current regional and global BVOC emission
645 models predict much smaller seasonal variations (Guenther et al., 2006, 2012; Muller et al.,
646 2008; Unger et al., 2013) compared to the measurements in Amazonia (Table 1).
647 Furthermore, satellite observations indicate that the current understanding of the processes
648 controlling seasonal variations is insufficient, and models do not simulate the unexpected
649 shutdown of isoprene emission in the Amazonia during the wet-to-dry transition season
650 (Barkley et al., 2009).

651 Many recently published studies have used the MEGAN model and the majority
652 have focused on improving our understanding of isoprene emissions. Although other
653 models have been developed on the basis of known biochemical processes (Grote et al.,
654 2014; Morfopoulos et al., 2014; Unger et al., 2013), the general framework and processes
655 simulated are similar. The biochemical basis of isoprene production and release must be
656 further understood to develop mechanistic explanations for variation in isoprene emission
657 (Monson et al., 2012), which may reduce uncertainties associated with the responses to
658 environmental factors.

659 Seasonal variation of isoprene emissions might be explained by the change in
660 energy supply from photosynthesis throughout the seasons (e.g. Grote et al., 2014). This is
661 supported by the generally strong correlation between isoprene emission and gross
662 photosynthetic capacity reported for Amazonian tree species (Kuhn et al., 2004b), and by
663 the fact that higher demography of healthy efficient leaves (Nelson et al., 2014) coincides
664 with the period of most efficient landscape-scale photosynthesis and photosynthetic
665 capacity (Restrepo-Coupe et al., 2013). However, more measurements are needed to
666 examine this relationship which should follow PAR variation. Additionally, since canopy

667 structure may explain some variation in biomass growth over tropical landscapes due to
668 differences in the pattern of light penetration and absorption by the canopies (Stark et al.,
669 2012), measurements of canopy structure may also help to explain some of the differences
670 in isoprenoid emissions among the Amazonian sub-regions.

671 Therefore, at least for the Amazonian rainforest, models currently do not fully
672 capture seasonal variations in isoprenoid emissions, especially for monoterpenes and
673 sesquiterpenes, which are less investigated compared to isoprene. The scarcity of
674 measurements in Amazonia prevents the development and evaluation of accurate model
675 approaches. Thus, this study strongly encourages future *in situ* measurements in Amazonia,
676 including at leaf level, in order to verify changes driven by seasonal variations in leaf area,
677 leaf age, phenology and emission response to soil moisture, and the short-term and long-
678 term temperature and light environment.
679

680 **4. Summary and conclusions**

681 In this study, we present the first in situ measurements that show a seasonal trend in
682 isoprenoid emissions for a primary rainforest of central Amazonia. Isoprenoid emissions
683 peak at the end of the dry season and at the dry-to-wet transition season. Under conditions
684 of high insolation and high temperatures joined together with the high demography of
685 photosynthetically efficient leaves (Caldararu et al., 2012; Myneni et al., 2007; Nelson et
686 al., 2014; Samanta et al., 2012), isoprenoid metabolic pathways may experience more
687 favorable conditions for synthesizing these compounds in the dry season and the dry-to-wet
688 transition season. This is especially for the case of isoprene and monoterpenes, which are
689 light- and temperature-dependent and are affected by the recent production of
690 photosynthetic substrates.

691 Although some studies have suggested that there are no seasonal variations in
692 canopy structure and greenness in Amazonia (e.g. Morton et al., 2014), results reported
693 here present a seasonal variation of leaf flushing and suggest maximum leaf demography in
694 the late dry season, which generally agrees with the assumption that a greenup during the
695 dry season in Amazonia may drive increasing isoprene emissions as suggested by satellite
696 retrievals (Barkley et al., 2009). Moreover, this study also suggests that seasonal changes in

697 the atmospheric oxidative capacity could have an important impact on the seasonality of at
698 least some isoprenoid concentrations and above canopy emissions, especially for
699 sesquiterpenes. Their quantification is challenged by rapid atmospheric chemical reactions
700 catalyzed by high insolation and higher ozone concentrations in the dry season.

701 MEGAN 2.1 estimates did not fully capture the behavior observed with the
702 isoprenoid emissions based on in-situ PTR-MS measurements (inverse Lagrangian
703 transport model). Model emissions of isoprene and total monoterpenes were overestimated,
704 especially during September 2010 (dry season) and December 2010 (wet season),
705 respectively. Total sesquiterpenes were underestimated during November 2010 (dry-to-wet
706 transition season). This difference between MEGAN 2.1 flux estimates and fluxes
707 estimated by the PTR-MS vertical mixing ratio profiles could be due to experimental errors
708 or the influence of very local effects on the seasonal emissions measured in this site,
709 because satellite-derived isoprene emissions agree fairly well with MEGAN 2.1 emission
710 estimates and the ground observations do not agree with the satellite data or the model,
711 principally in September. Perhaps the isoprene pattern observed at the site is due to a very
712 local effect of leaf flushing by isoprene emitting species around this tower, but this is not
713 seen on the regional scale where there are different species distributions.

714 Generally, current models assume that seasonal variation of BVOC emissions in the
715 Amazonian rainforest are primarily based on light and temperature variations. These model
716 simulations capture only a part of the actual variation and have uncertainties associated
717 with the insufficient understanding of mechanistic processes involved in the seasonality of
718 these compounds. Nevertheless, because the number of measurements and sites is limited in
719 Amazonia, there is a scarcity of information, which hinders further model improvements. In
720 summary, our results demonstrate strong seasonality and suggest that important processes
721 are taking place during the transition seasons. Also, results reveal the need for long-term
722 and continuous BVOC observations from leaf level to ecosystem level, and also suggest
723 that standardized measurement procedures are required in order to compare the different
724 Amazonian sub-regions. This may advance understanding of the seasonality of BVOC
725 exchanges between forest and atmosphere, providing the information needed to improve
726 BVOC emission estimates for climate and air quality modelling studies.
727

Acknowledgements

This work was performed at the National Institute for Amazon Research and at the State University of Amazonas with funding provided by the CNPq (fellowship provided to E. Alves by the Brazilian government), and financial support for field work was provided by the Philecology Foundation of Fort Worth, Texas, and the National Science Foundation through the AMAZON-PIRE (Partnerships for International Research and Education) award (0730305) and instrumentation support (CHE 0216226). We also thank Dr. Scott Saleska for supporting this long field campaign. This research was also supported by the Office of Biological and Environmental Research of the U.S. Department of Energy under Contract No. DE-AC02-05CH11231 as part of their Terrestrial Ecosystem Science Program. The authors would like to acknowledge the advice and support from the Large Biosphere-Atmosphere (LBA) as a part of the Green Ocean Amazon (GoAmazon) 2014/5 project in Manaus, Brazil.T. Stavrakou was supported by the GlobEmission project (No 4000104001/11/I-NB) of the European Space Agency.

References

Ahlm, L., Nilsson, E. D., Krejci, R., Mårtensson, E. M., Vogt, M. and Artaxo, P.: A comparison of dry and wet season aerosol number fluxes over the Amazon rain forest, Atmos. Chem. Phys., 10(6), 3063–3079, doi:10.5194/acp-10-3063-2010, 2010.

Alves, E. G., Harley, P., Gonçalves, J. F. D. C., Eduardo, C. and Jardine, K.: Effects of light and temperature on isoprene emission at different leaf developmental stages of Eschweilera coriacea in central Amazon, Acta Amaz., 44(1), 9–18, doi: 10.1590/S0044-59672014000100002, 2014.

Andreae, M. O., Artaxo, P., Brandao, C., Carswell, F. E., Ciccioli, P., da Costa, A. L., Culf, A. D., Esteves, J. L., Gash, J. H. C., Grace, J., Kabat, P., Lelieveld, J., Malhi, Y., Manzi, A. O., Meixner, F. X., Nobre, A. D., Nobre, C., Ruivo, M., Silva-Dias, M. A., Stefani, P., Valentini, R., von Jouanne, J. and Waterloo, M. J.: Biogeochemical cycling of carbon, water, energy, trace gases, and aerosols in Amazonia: The LBA-EUSTACH experiments, J. Geophys. Res., 107(D20), doi: 8066 10.1029/2001jd000524, 2002.

Aquino, C. A. B.: Identificação de Compostos Orgânicos Voláteis (COVs) emitidos por Florestas na região Amazônica [*in Portuguese*], Master thesis. Federal University of Mato Grosso, Cuiabá-MT, Brazil, 106 pp., 2006.

Araujo, A. C., Nobre, A. D., Kruijt, B., Elbers, J. A., Dallarosa, R., Stefani, P., von Randow, C., Manzi, A. O., Culf, A. D., Gash, J. H. C., Valentini, R., Kabat, P. and Araújo, A. C.: Comparative measurements of

759 carbon dioxide fluxes from two nearby towers in a central Amazonian rainforest: The Manaus LBA site, J.
760 Geophys. Res., 107(D20), 8090, doi:8090 10.1029/2001jd000676, 2002.

761 Arneth, A., Monson, R. K., Schurgers, G., Niinemets, U. and Palmer, P. I.: Why are estimates of global
762 terrestrial isoprene emissions so similar (and why is this not so for monoterpenes)?, Atmos. Chem. Phys.,
763 8(16), 4605–4620, doi:10.5194/acp-8-4605-2008, 2008.

764 Arneth, A., Niinemets, U., Pressley, S., Back, J., Hari, P., Karl, T., Noe, S., Prentice, I. C., Serca, D., Hickler,
765 T., Wolf, A. and Smith, B.: Process-based estimates of terrestrial ecosystem isoprene emissions: incorporating
766 the effects of a direct CO_2-isoprene interaction, Atmos. Chem. Phys., 7, 31–53, doi:10.5194/acp-7-31-2007,
767 2007.

768 Atkinson, R. and Arey, J.: Atmospheric Degradation of Volatile Organic Compounds, Chem. Rev., 103(3),
769 4605–4638, doi:10.1021/cr0206420, 2003.

770 Austin, A. T., Vivanco, L., González-Arzac, A. and Pérez, L. I.: There's no place like home? An exploration
771 of the mechanisms behind plant litter-decomposer affinity in terrestrial ecosystems, New Phytol., 204(2),
772 307–314, doi:10.1111/nph.12959, 2014.

773 Barkley, M. P., Palmer, P. I., Kuhn, U., Kesselmeier, J., Chance, K., Kurosu, T. P., Martin, R. V., Helmig, D.
774 and Guenther, A.: Net ecosystem fluxes of isoprene over tropical South America inferred from Global Ozone
775 Monitoring Experiment (GOME) observations of HCHO columns, J. Geophys. Res., 113(D20), D20304,
776 doi:10.1029/2008JD009863, 2008.

777 Barkley, M. P., Palmer, P. I., De Smedt, I., Karl, T., Guenther, A. and Van Roozendael, M.: Regulated large-
778 scale annual shutdown of Amazonian isoprene emissions?, Geophys. Res. Lett., 36(4), L04803,
779 doi:10.1029/2008GL036843, 2009.

780 Barkley, M. P., Smedt, I. De, Van Roozendael, M., Kurosu, T. P., Chance, K., Arneth, A., Hagberg, D.,
781 Guenther, A., Paulot, F., Marais, E. and Mao, J.: Top-down isoprene emissions over tropical South America
782 inferred from SCIAMACHY and OMI formaldehyde columns, J. Geophys. Res. Atmos., 118(12), 6849–
783 6868, doi:10.1002/jgrd.50552, 2013.

784 Bauwens, M., Stavrakou, T., Müller, J. F., De Smedt, I., Van Roosendael, M.: Satellite-based isoprene
785 emission estimates (2007-2012) from the GlobEmission projet, ACCENT-Plus Symposium, Atmospheric
786 Composition Change: the European Network", Urbino, 17-20 September, 2013.

787 Bracho-Nunez, A., Knothe, N. M., Welter, S., Staudt, M., Costa, W. R., Liberato, M. A. R., Piedade, M. T. F.
788 and Kesselmeier, J.: Leaf level emissions of volatile organic compounds (VOC) from some Amazonian and
789 Mediterranean plants, Biogeosciences, 10(9), 5855–5873, doi:10.5194/bg-10-5855-2013, 2013.

790 Caldararu, S., Palmer, P. I. and Purves, D. W.: Inferring Amazon leaf demography from satellite observations
791 of leaf area index, Biogeosciences, 9(4), 1389–1404, doi:10.5194/bg-9-1389-2012, 2012.

792 Ciccioli, P., Brancaleoni, E., Frattoni, M., Kuhn, U., Kesselmeir, J., Dindorf, T., De Araujo, A. C., Nobre, A.
793 D., Stefani, P. and Velentini, R.: Fluxes of isoprenoid compounds over the tropical rainforest near Manaus
794 during the dry season and their implications in the ecosystem carbon budget and in the atmospheric chemistry
795 processes, Report Series in Aerosol Science (62A) Proceedings of Integrated Land Ecosystem Atmosphere
796 Processes Study (ILEAPS) International Open Science Conference, Helsinki, Finland, 29 September – 3
797 October, ISBN 952 -5027-40-6, 2003.

798 Cleveland, C. C. and Yavitt, J. B.: Consumption of atmospheric isoprene in soil, Geophys. Res. Lett., 24(19),
799 2379–2382, doi:10.1029/97GL02451, 1997.

800 Cuartas, L. A., Tomasella, J., Nobre, A. D., Nobre, C. A., Hodnett, M. G., Waterloo, M. J., Oliveira, S. M.
801 De, Randow, R. D. C. Von, Trancoso, R. and Ferreira, M.: Distributed hydrological modeling of a micro-
802 scale rainforest watershed in Amazonia: Model evaluation and advances in calibration using the new HAND
803 terrain model, J. Hydrol., 462-463, 15–27, doi:10.1016/j.jhydrol.2011.12.047, 2012.

804 da Rocha, H. R., Manzi, A. O., Cabral, O. M., Miller, S. D., Goulden, M. L., Saleska, S. R., R.-Coupe, N.,
805 Wofsy, S. C., Borma, L. S., Artaxo, P., Vourlitis, G., Nogueira, J. S., Cardoso, F. L., Nobre, A. D., Kruijt, B.,
806 Freitas, H. C., von Randow, C., Aguiar, R. G. and Maia, J. F.: Patterns of water and heat flux across a biome
807 gradient from tropical forest to savanna in Brazil, J. Geophys. Res., 114, G00B12,
808 doi:10.1029/2007JG000640, 2009.

809 Davis, K. J., Lenschow, D. H. and Zimmerman, P. R.: Biogenic nonmethane hydrocarbon emissions
810 estimated from tethered balloon observations, J. Geophys. Res., 99(D12), 25587, doi:10.1029/94JD02009,
811 1994.

812 Duhl, T. R., Helmig, D. and Guenther, A.: Sesquiterpene emissions from vegetation: a review,
813 Biogeosciences, 5(3), 761–777, doi:10.5194/bg-5-761-2008, 2008.

814 Fidelis, C. H. V., Augusto, F., Sampaio, P. T. B., Krainovic, P. M. and Barata, L. E. S.: Chemical
815 characterization of rosewood (*Aniba rosaeodora* Ducke) leaf essential oil by comprehensive two-
816 dimensional gas chromatography coupled with quadrupole mass spectrometry, J. Essent. Oil Res., 24(3), 245–
817 251, doi:10.1080/10412905.2012.676770, 2012.

818 Geron, C., Rasmussen, R., R. Arnts, R. and Guenther, A.: A review and synthesis of monoterpene speciation
819 from forests in the United States, Atmos. Environ., 34(11), 1761–1781, doi:10.1016/S1352-2310(99)00364-7,
820 2000.

821 Goldan, P. D., Kuster, W. C., Fehseneld, F. C. and Montzka, S. A.: Hydrocarbon measurements in the
822 southeastern United States: The Rural Oxidants in the Southern Environment (ROSE) Program 1990, J.
823 Geophys. Res., 100, 25945, doi:10.1029/95JD02607,1995.

824 Goldstein, A. H. and Galbally, I. E.: Known and Unexplored Organic Constituents in the Earth's Atmosphere,
825 Environ. Sci. Technol., 41(5), 1514–1521, doi:10.1021/es072476p, 2007.

826 Gray, C. M., Monson, R. K. and Fierer, N.: Biotic and abiotic controls on biogenic volatile organic compound
827 fluxes from a subalpine forest floor, J. Geophys. Res. Biogeosciences, 119(4), 547–556,
828 doi:10.1002/2013JG002575, 2014.

829 Greenberg, J. P., Guenther, A. B., Petron, G., Wiedinmyer, C., Vega, O., Gatti, L. V, Tota, J. and Fisch, G.:
830 Biogenic VOC emissions from forested Amazonian landscapes, Glob. Chang. Biol., 10(5), 651–662,
831 doi:10.1111/j.1529-8817.2003.00758.x, 2004.

832 Greenberg, J. P. and Zimmerman, P. R.: Nonmethane hydrocarbons in remote tropical, continental, and
833 marine atmospheres, J. Geophys. Res., 89(D3), 4767, doi:10.1029/JD089iD03p04767, 1984.

834 Grote, R., Morfopoulos, C., Niinemets, Ü., Sun, Z., Keenan, T. F., Pacifico, F. and Butler, T.: A fully
835 integrated isoprenoid emissions model coupling emissions to photosynthetic characteristics., Plant. Cell
836 Environ., 37(8), 1965–80, doi:10.1111/pce.12326, 2014.

837 Guenther, A. B., Jiang, X., Heald, C. L., Sakulyanontvittaya, T., Duhl, T., Emmons, L. K. and Wang, X.: The
838 Model of Emissions of Gases and Aerosols from Nature version 2.1 (MEGAN2.1): an extended and updated
839 framework for modeling biogenic emissions, Geosci. Model Dev., 5(2), 1503–1560, doi:10.5194/gmdd-5-
840 1503-2012, 2012.

841 Guenther, A., Karl, T., Harley, P., Wiedinmyer, C., Palmer, P. I. and Geron, C.: Estimates of global terrestrial
842 isoprene emissions using MEGAN (Model of Emissions of Gases and Aerosols from Nature), Atmos. Chem.
843 Phys., 6(1), 3181–3210, doi:10.5194/acpd-6-107-2006, 2006.

844 Guenther, A.: The contribution of reactive carbon emissions from vegetation to the carbon balance of
845 terrestrial ecosystems, Chemosphere, 49(8), 837–44, doi:10.1016/S0045-6535(02)00384-3, 2002.

846 Guenther, A. B.: Upscaling biogenic volatile compound emissions from leaves to landscapes, in Biology,
847 controls and models of tree volatile organic compound emissions, edited by Ü. Niinemets and R. K. Monson,
848 pp. 391–414, Springer, Berlin., 2013.

849 Hamba, A.: Modified K model for chemically reactive species in the planetary boundary layer. J. Geophys.
850 Res., 98 (D3), 5173–5182, doi:10.1029/92JD02511, 1993.

851 Hanna, S. R., Russel, A. G., Wilkinson, J. G., Vukovich, Hansen, D. A.: Monte Carlo estimation of
852 uncertainties in BEIS3 emission outputs and their effects on uncertainties in chemical transport model
853 predictions. J. Geophys. Res., 110 (D01302), doi:10.1029/2004JD004986, 2005.

854 Harley, P., Vasconcellos, P., Vierling, L., Pinheiro, C. C. D. S., Greenberg, J., Guenther, A., Klinger, L.,
855 Almeida, S. S. De, Neill, D., Baker, T., Phillips, O., Malhi, Y. and De Almeida, S. S.: Variation in potential
856 for isoprene emissions among Neotropical forest sites, Glob. Chang. Biol., 10(5), 630–650,
857 doi:10.1111/j.1529-8817.2003.00760.x, 2004.

858 Helmig, D., Balsley, B., Kuck, R., Jensen, M., Smith, T. and Birks, J. W.: Vertical profiling and
859 determination of landscape fluxes of biogenic nonmethane hydrocarbons within the planetary boundary layer
860 in the Peruvian Amazon, J. Geophys. Res., 103(98), 519–532, doi:10.1029/98JD01023, 1998.

861 Jacob, D. J. and Wofsy, S. C.: Photochemistry of biogenic emissions over the Amazon forest, J. Geophys.
862 Res., 93(D2), 1477–1486, doi:10.1029/JD093iD02p01477, 1988.

863 Jardine, A. B., Jardine, K. J., Fuentes, J. D., Martin, S. T., Martins, G., Durgante, F., Carneiro, V., Higuchi,
864 N., Manzi, A. O. and Chambers, J. Q.: Highly reactive light-dependent monoterpenes in the Amazon,
865 Geophys. Res. Lett., 42, 1-8, doi: 10.1002/2014GL062573, 2015.

866 Jardine, K. J., Henderson, W. M., Huxman, T. E. and Abrell, L.: Dynamic Solution Injection: a new method
867 for preparing pptv–ppbv standard atmospheres of volatile organic compounds, Atmos. Meas. Tech., 3(6),
868 1569–1576, doi:10.5194/amt-3-1569-2010, 2010.

869 Jardine, K. J., Monson, R. K., Abrell, L., Saleska, S. R., Arneth, A., Jardine, A., Ishida, F. Y., Serrano, A. M.
870 Y., Artaxo, P., Karl, T., Fares, S., Goldstein, A., Loreto, F. and Huxman, T.: Within-plant isoprene oxidation
871 confirmed by direct emissions of oxidation products methyl vinyl ketone and methacrolein, Glob. Chang.
872 Biol., 18(3), 973–984, doi:10.1111/j.1365-2486.2011.02610.x, 2012.

873 Jardine, K., Yañez Serrano, A., Arneth, A., Abrell, L., Jardine, A., van Haren, J., Artaxo, P., Rizzo, L. V.,
874 Ishida, F. Y., Karl, T., Kesselmeier, J., Saleska, S. and Huxman, T.: Within-canopy sesquiterpene ozonolysis
875 in Amazonia, J. Geophys. Res., 116(D19), D19301, doi:10.1029/2011jd016243, 2011.

876 Jones, M. O., Kimball, J. S. and Nemani, R. R.: Asynchronous Amazon forest canopy phenology indicates
877 adaptation to both water and light availability, Environ. Res. Lett., 9(12), 124021, doi:10.1088/1748-
878 9326/9/12/124021, 2014.

879 Karl, T., Guenther, A., Turnipseed, A., Tyndall, G., Artaxo, P. and Martin, S.: Rapid formation of isoprene
880 photo-oxidation products observed in Amazonia, Atmos. Chem. Phys., 9(20), 7753–7767, doi:10.5194/acp-9-
881 7753-2009, 2009.

882 Karl, T., Guenther, A., Yokelson, R. J., Greenberg, J., Potosnak, M., Blake, D. R. and Artaxo, P.: The tropical
883 forest and fire emissions experiment: Emission, chemistry, and transport of biogenic volatile organic
884 compounds in the lower atmosphere over Amazonia, J. Geophys. Res., 112(D18), D18302,
885 doi:10.1029/2007JD008539, 2007.

886 Karl, T., Harley, P., Emmons, L., Thornton, B., Guenther, A., Basu, C., Turnipseed, A. and Jardine, K.:
887 Efficient Atmospheric Cleansing of Oxidized Organic Trace Gases by Vegetation, Science, 330(6005), 816–
888 819, doi:10.1126/science.1192534, 2010.

889 Karl, T., Potosnak, M., Guenther, A. B., Clark, D., Walker, J., Herrick, J. D. and Geron, C.: Exchange
890 processes of volatile organic compounds above a tropical rain forest: Implications for modeling tropospheric
891 chemistry above dense vegetation, J. Geophys. Res., 109(D18), D18306, doi:10.1029/2004JD004738, 2004.

892 Kesselmeier, J., Kuhn, U., Rottenberger, S., Biesenthal, T., Wolf, A., Schebeske, G., Andreae, M. O.,
893 Ciccioli, P., Brancaleoni, E., Frattoni, M., Oliva, S. T., Botelho, M. L., Silva, C. M. A. and Tavares, T. M.:
894 Concentrations and species composition of atmospheric volatile organic compounds (VOCs) as observed
895 during the wet and dry season in Rondônia (Amazonia), J. Geophys. Res., 107(D20), 8053,
896 doi:10.1029/2000JD000267, 2002.

897 Kesselmeier, J., Kuhn, U., Wolf, A., Andreae, M., Ciccioli, P., Brancaleoni, E., Frattoni, M., Guenther, A.,
898 Greenberg, J., De Castro Vasconcellos, P., de Oliva, T., Tavares, T. and Artaxo, P.: Atmospheric volatile
899 organic compounds (VOC) at a remote tropical forest site in central Amazonia, Atmos. Environ., 34(24),
900 4063–4072, doi:10.1016/S1352-2310(00)00186-2, 2000.

901 Kuhn, U., Andreae, M. O., Ammann, C., Araújo, A. C., Brancaleoni, E., Ciccioli, P., Dindorf, T., Frattoni,
902 M., Gatti, L. V., Ganzeveld, L., Kruijt, B., Lelieveld, J., Lloyd, J., Meixner, F. X., Nobre, A. D., Pöschl, U.,
903 Spirig, C., Stefani, P., Thielmann, A., Valentini, R. and Kesselmeier, J.: Isoprene and monoterpene fluxes
904 from Central Amazonian rainforest inferred from tower-based and airborne measurements, and implications
905 on the atmospheric chemistry and the local carbon budget, Atmos. Chem. Phys., 7(1), 641–708,
906 doi:10.5194/acpd-7-641-2007, 2007.

907 Kuhn, U., Rottenberger, S., Biesenthal, T., Wolf, a., Schebeske, G., Ciccioli, P., Brancaleoni, E., Frattoni, M.,
908 Tavares, T. M. and Kesselmeier, J.: Seasonal differences in isoprene and light-dependent monoterpene
909 emission by Amazonian tree species, Glob. Chang. Biol., 10(5), 663–682, doi:10.1111/j.1529-
910 8817.2003.00771.x, 2004a.

911 Kuhn, U., Rottenberger, S., Biesenthal, T., Wolf, A., Schebeske, G., Ciccioli, P., Brancaleoni, E., Frattoni,
912 M., Tavares, T. M. and Kesselmeier, J.: Isoprene and monoterpene emissions of Amazonian tree species
913 during the wet season: Direct and indirect investigations on controlling environmental functions, J. Geophys.
914 Res., 107(D20), 8071, doi:8071 10.1029/2001jd000978, 2002.

915 Kuhn, U., Rottenberger, S., Biesenthal, T., Wolf, A., Schebeske, G., Ciccioli, P. and Kesselmeier, J.: Strong
916 correlation between isoprene emission and gross photosynthetic capacity during leaf phenology of the tropical
917 tree species *Hymenaea courbaril* with fundamental changes in volatile organic compounds emission
918 composition during early leaf development, Plant, Cell Environ., 27(12), 1469–1485, doi:10.1111/j.1365-
919 3040.2004.01252.x, 2004b.

920 Lamb, B., Guenther, A., Gay, D., Westberg, H.: A National Inventory of Biogenic Hydrocarbon Emissions.
921 Atmos. Environ., 21(8): 1695-1705, doi:10.1016/0004-6981(87)90108-9, 1987.

922 Lamb, B., Pierce, T., Baldocchi, D., Allwine, E., Dilts, S., Westberg, H., Geron, C., Guenther, A., Klinger, L.,
923 Harley, P., Zimmerman, P.: Evaluation of forest canopy models for estimating isoprene emissions. J.
924 Geophys. Res., 101(D17): 22787-22797, doi:10.1029/96JD00056, 1996.

925 Laothawornkitkul, J., Taylor, J. E., Paul, N. D. and Hewitt, C. N.: Biogenic volatile organic compounds in the
926 Earth system, New Phytol., 183(1), 27–51, doi:10.1111/j.1469-8137.2009.02859.x, 2009.

927 Lelieveld, J., Butler, T. M., Crowley, J. N., Dillon, T. J., Fischer, H., Ganzeveld, L., Harder, H., Lawrence, M.
928 G., Martinez, M., Taraborrelli, D. and Williams, J.: Atmospheric oxidation capacity sustained by a tropical
929 forest, Nature, 452(7188), 737–40, doi:10.1038/nature06870, 2008.

930 Lima, P., Zoghbi, G. B., Andrade, E. H. A., D, T. M., Fernandes, C. S., Lauraceae, B. and Words, K. E. Y.:
931 Constituintes voláteis das folhas e dos galhos de Cinnamomum zeylanicum Blume (Lauraceae) Volatile
932 constituents from leaves and branches of, Acta Amaz., 35(3), 363–366, 2005.

933 Lindinger, W., Hansel, A. and Jordan, A.: On-line monitoring of volatile organic compounds at pptv levels by
934 means of proton-transfer-reaction mass spectrometry (PTR-MS) medical applications, food control and
935 environmental research, Int. J. Mass Spectrom. Ion Process., 173(3), 191–241,
936 doi:http://dx.doi.org/10.1016/S0168-1176(97)00281-4, 1998.

937 Liu, Y. J., Herdlinger-Blatt, I., McKinney, K. a. and Martin, S. T.: Production of methyl vinyl ketone and
938 methacrolein via the hydroperoxyl pathway of isoprene oxidation, Atmos. Chem. Phys., 13, 5715–5730,
939 doi:10.5194/acp-13-5715-2013, 2013.

940 Loreto, F., Ciccioli, P., Cecinato, A., Brancaleoni, E., Frattoni, M., Fabozzi, C., Tricoli, D., C, C. I. A. P. and
941 Salaria, V.: Evidence of the Photosynthetic Origin of Monoterpenes Emitted by Quercus ilex L . Leaves by
942 I3C Labeling, Plant Physiol., 110(1996), 1317–1322, 1996.

943 Loreto, F. and Velikova, V.: Isoprene produced by leaves protects the photosynthetic apparatus against ozone
944 damage, quenches ozone products, and reduces lipid peroxidation of cellular membranes, Plant Physiol.,
945 127(4), 1781–7, doi:10.1104/pp.010497., 2001.

946 Luizão, F. J.: Litter production and mineral element input to the forest floor in a central Amazonian forest,
947 GeoJournal, 19(4), 407-417, 1989.

948 Malhi, Y., Aragão, L. E. O. C., Metcalfe, D. B., Paiva, R., Quesada, C. A., Almeida, S., Anderson, L.,
949 Brando, P., Chambers, J. Q., da COSTA, A. C. L., Hutyra, L. R., Oliveira, P., Patiño, S., Pyle, E. H.,
950 Robertson, A. L. and Teixeira, L. M.: Comprehensive assessment of carbon productivity, allocation and
951 storage in three Amazonian forests, Glob. Chang. Biol., 15(5), 1255–1274, doi:10.1111/j.1365-
952 2486.2008.01780.x, 2009.

953 Marengo, J. A., Nobre, C. A., Tomasella, J., Oyama, M. D., Sampaio de Oliveira, G., de Oliveira, R.,
954 Camargo, H., Alves, L. M. and Brown, I. F.: The Drought of Amazonia in 2005, J. Clim., 21(3), 495–516,
955 doi:10.1175/2007JCLI1600.1, 2008.

956 Marengo, J. A., Tomasella, J., Alves, L. M., Soares, W. R. and Rodriguez, D. A.: The drought of 2010 in the
957 context of historical droughts in the Amazon region, Geophys. Res. Lett., 38(12), 1-5,
958 doi:10.1029/2011GL047436, 2011.

959 Martin, S. T., Andreae, M. O., Althausen, D., Artaxo, P., Baars, H., Borrmann, S., Chen, Q., Farmer, D. K.,
960 Guenther, A., Gunthe, S. S., Jimenez, J. L., Karl, T., Longo, K., Manzi, A., Muller, T., Pauliquevis, T.,

961 Petters, M. D., Prenni, A. J., Poschl, U., Rizzo, L. V, Schneider, J., Smith, J. N., Swietlicki, E., Tota, J.,
962 Wang, J., Wiedensohler, A. and Zorn, S. R.: An overview of the Amazonian Aerosol Characterization
963 Experiment 2008 (AMAZE-08), Atmos. Chem. Phys., 10(23), 11415–11438, doi:10.5194/acp-10-11415-
964 2010, 2010.

965 Misztal, P. K., Karl, T., Weber, R., Jonsson, H. H., Guenther, A. B., Goldstein, A., H.: Airborne flux
966 measurements of biogenic isoprene over California. Atmos. Chem. Phys, 14(19): 10631-10647,
967 doi:10.5194/acp-14-10631-2014, 2014.

968 MODIS-NASA: Leaf Area Index - Fraction Photosynth. Act. Radiat. 8-Day L4 Glob. 1km [online] Available
969 from: https://lpdaac.usgs.gov/dataset_discovery/modis/modis_products_table/mcd15a2, 2015.

970 Monson, R. K., Grote, R., Niinemets, Ü. and Schnitzler, J.-P.: Modeling the isoprene emission rate from
971 leaves, 195, 541–559, doi:10.1111/j.1469-8137.2012.04204.x, 2012.

972 Morfopoulos, C., Prentice, I. C., Keenan, T. F., Friedlingstein, P., Medlyn, B. E., Peñuelas, J. and Possell, M.:
973 A unifying conceptual model for the environmental responses of isoprene emissions from plants, Ann. Bot.,
974 112(7), 1223–38, doi:10.1093/aob/mct206, 2013.

975 Morfopoulos, C., Sperlich, D., Pe, J., Filella, I., Llusi, J., Possell, M., Sun, Z., Prentice, I. C. and Medlyn, B.
976 E.: A model of plant isoprene emission based on available reducing power captures responses to atmospheric
977 CO_2, New Phytol., 203 , 125–139, doi: 10.1111/nph.12770,2014.

978 Morton, D. C., Nagol, J., Carabajal, C. C., Rosette, J., Palace, M., Cook, B. D., Vermote, E. F., Harding, D. J.
979 and North, P. R. J.: Amazon forests maintain consistent canopy structure and greenness during the dry season,
980 Nature, 506(7487), 221–4, doi:10.1038/nature13006, 2014.

981 Müller, J. F., Stavrakou, T., Wallens, S., De Smedt, I., Van Roozendael, M., Potosnak, M. J., Rinne, J.,
982 Munger, B., Goldstein, A., Guenther, A. B., Smedt, I. De and Roozendael, M. Van: Global isoprene emissions
983 estimated using MEGAN, ECMWF analyses and a detailed canopy environment model, Atmos. Chem. Phys.,
984 8(5), 1329–1341, doi:10.5194/acp-8-1329-2008, 2008.

985 Myneni, R. B., Yang, W., Nemani, R. R., Huete, A. R., Dickinson, R. E., Knyazikhin, Y., Didan, K., Fu, R.,
986 Negrón Juárez, R. I., Saatchi, S. S., Hashimoto, H., Ichii, K., Shabanov, N. V, Tan, B., Ratana, P., Privette, J.
987 L., Morisette, J. T., Vermote, E. F., Roy, D. P., Wolfe, R. E., Friedl, M. A., Running, S. W., Votava, P., El-
988 Saleous, N., Devadiga, S., Su, Y. and Salomonson, V. V: Large seasonal swings in leaf area of Amazon
989 rainforests, Proc. Natl. Acad. Sci. U. S. A., 104(12), 4820–4823, doi:10.1073/pnas.0611338104, 2007.

990 Nelson, B., Tavares, J., Wu, J., Valeriano, D., Lopes, A., Marostica, S., Martins, G., Prohaska, N., Albert, L.,
991 De Araújo, A., Manzi, A., Saleska, S., Huete, A.: Seasonality of central Amazon Forest Leaf Flush using
992 tower mounted RGB Camera, AGU Fall Meeting, San Francisco, California, 15-19 December, B11G-0107,
993 2014.

994 Nemitz, E., Sutton, M. A., Gut, A., San José, R., Husted, S. and Schjoerring, J. K.: Sources and sinks of
995 ammonia within an oilseed rape canopy, Agric. For. Meteorol., 105(4), 385–404, doi:10.1016/S0168-
996 1923(00)00205-7, 2000.

997 Oliveira, A. N. De, Braule, M., Ramos, P., Couto, L. B. and Sahdo, R. M.: Composição e diversidade
998 florístico-estrutural de um hectare de floresta densa de terra firme na Amazônia, Acta Amaz., 38(4), 627–642,
999 doi: 10.1590/S0044-59672008000400005, 2008.

1000 Park, J.-H., Goldstein, A. H., Timkovsky, J., Fares, S., Weber, R., Karlik, J. and Holzinger, R.: Active
1001 atmosphere-ecosystem exchange of the vast majority of detected volatile organic compounds, Science,
1002 341(6146), 643–647, doi:10.1126/science.1235053, 2013.

1003 Parker, G., and D. R. Fitzjarrald.: Canopy structure and radiation environment metrics indicate forest
1004 developmental stage, disturbance, and certain ecosystem functions, III LBA Scientific Conference, Braz.
1005 Minist. of Sci. and Technol., Brasilia, Brazil, 27-29 July, 2004.

1006 Pires, J. M. and Prance, G. T.: Key environments: Amazonia, in Vegetation types of the Brazilian Amazonia.,
1007 edited by G. T. Prance and T. E. Lovejoy, Pergamon, New York., 1985.

1008 Rasmussen, R. A. and Khalil, M. A. K.: Isoprene over the Amazon Basin, J. Geophys. Res., 93(D2), 1417,
1009 doi:10.1029/JD093iD02p01417, 1988.

1010 Raupach, M.: Applying Lagrangian Fluid Mechanics to infer scalar source distributions from concentration
1011 profiles in plant canopies, Agric. For. Meteorol., 47, 85–108, doi:10.1016/0168-1923(89)90089-0,1989.

1012 Restrepo-Coupe, N., da Rocha, H. R., Hutyra, L. R., da Araujo, A. C., Borma, L. S., Christoffersen, B.,
1013 Cabral, O. M. R. R., de Camargo, P. B., Cardoso, F. L., da Costa, A. C. L., Fitzjarrald, D. R., Goulden, M. L.,
1014 Kruijt, B., Maia, J. M. F. F., Malhi, Y. S., Manzi, A. O., Miller, S. D., Nobre, A. D., von Randow, C., Sá, L.
1015 D. A., Sakai, R. K., Tota, J., Wofsy, S. C., Zanchi, F. B. and Saleska, S. R.: What drives the seasonality of
1016 photosynthesis across the Amazon basin? A cross-site analysis of eddy flux tower measurements from the
1017 Brasil flux network, Agric. For. Meteorol., 182-183, 128–144, doi:10.1016/j.agrformet.2013.04.031, 2013.

1018 Rinne, H. J. I., Guenther, A. B., Greenberg, J. P. and Harley, P. C.: Isoprene and monoterpene fluxes
1019 measured above Amazonian rainforest and their dependence on light and temperature, Atmos. Environ.,
1020 36(14), 2421–2426, doi:10.1016/S1352-2310(01)00523-4, 2002.

1021 Rizzo, L. V. V, Artaxo, P., Karl, T., Guenther, A. B. B. and Greenberg, J.: Aerosol properties, in-canopy
1022 gradients, turbulent fluxes and VOC concentrations at a pristine forest site in Amazonia, Atmos. Environ.,
1023 44(4), 503–511, doi:10.1016/j.atmosenv.2009.11.002, 2010.

1024 Samanta, A., Knyazikhin, Y., Xu, L., Dickinson, R. E., Fu, R., Costa, M. H., Saatchi, S. S., Nemani, R. R. and
1025 Myneni, R. B.: Seasonal changes in leaf area of Amazon forests from leaf flushing and abscission, J.
1026 Geophys. Res. Biogeosciences, 117(G1), n/a–n/a, doi:10.1029/2011JG001818, 2012.

1027 Silva, C. P.: Estudos observacionais das principais fontes de emissão de compostos orgânicos voláteis (VOC)
1028 em floresta intacta de terra firme na Amazônia Central [*in Portuguese*], Master thesis. National Institute for
1029 Amazon Research, Manaus-AM, Brazil, 91 pp., 2010.

1030 Silva, F. B., Shimabukuro, Y. E., Aragão, L. E. O. C., Anderson, L. O., Pereira, G., Cardozo, F. and Arai, E.:
1031 Corrigendum: Large-scale heterogeneity of Amazonian phenology revealed from 26-year long
1032 AVHRR/NDVI time-series, Environ. Res. Lett., 8(2), 029502, doi:10.1088/1748-9326/8/2/029502, 2013.

1033 Simon, E., Meixner, F. X., Rummel, U., Ganzeveld, L., Ammann, C. and Kesselmeier, J.: Coupled carbon-
1034 water exchange of the Amazon rain forest, II. Comparison of predicted and observed seasonal exchange of
1035 energy, CO_2, isoprene and ozone at a remote site in Rondonia, Biogeosciences, 2(3), 255–275,
1036 doi:10.5194/bg-2-255-2005, 2005.

1037 Stark, S. C., Leitold, V., Wu, J. L., Hunter, M. O., de Castilho, C. V, Costa, F. R. C., McMahon, S. M.,
1038 Parker, G. G., Shimabukuro, M. T., Lefsky, M. a, Keller, M., Alves, L. F., Schietti, J., Shimabukuro, Y. E.,
1039 Brandão, D. O., Woodcock, T. K., Higuchi, N., de Camargo, P. B., de Oliveira, R. C., Saleska, S. R. and
1040 Chave, J.: Amazon forest carbon dynamics predicted by profiles of canopy leaf area and light environment.,
1041 Ecol. Lett., 15(12), 1406–14, doi:10.1111/j.1461-0248.2012.01864.x, 2012.

1042 Stavrakou, T., Müller, J.-F., Bauwens, M., De Smedt, I., Van Roozendael, M., De Mazière, M., Vigouroux,
1043 C., Hendrick, F., George, M., Clerbaux, C., Coheur, P.-F. and Guenther, A.: How consistent are top-down
1044 hydrocarbon emissions based on formaldehyde observations from GOME-2 and OMI? Atmos. Chem. Phys.
1045 Discuss., 15, 12007-12067, doi:10.5194/acpd-15-12007-2015, 2015.

1046 Stavrakou, T., Müller, J.-F., Bauwens, M., De Smedt, I., Van Roozendael, M., Guenther, A., Wild, M. and
1047 Xia, X.: Isoprene emissions over Asia 1979–2012: impact of climate and land-use changes, Atmos. Chem.
1048 Phys., 14(9), 4587–4605, doi:10.5194/acp-14-4587-2014, 2014.

1049 Stavrakou, T., Müller, J.-F., De Smedt, I., Van Roozendael, M., van der Werf, G. R., Giglio, L. and Guenther,
1050 a.: Global emissions of non-methane hydrocarbons deduced from SCIAMACHY formaldehyde columns
1051 through 2003–2006, Atmos. Chem. Phys., 9, 3663-3679, 2009, doi:10.5194/acp-9-3663-2009, 2009.

1052 Stefani,P.: Preliminary assessment of VOC fluxes form a primary rain forest performed in the LBA site at
1053 Manaus, I LBA Scientific Conference, Braz. Minist. of Sci. and Technol., Belém, Brazil, 2-4 June, 2000.

1054 Tavares, J. V.: Green-up na Estação Seca da Amazônia Central: Padrões sazonais da fenologia foliar de uma
1055 floresta de terra firme [*in Portuguese*]. Master thesis. National Institute for Amazon Research, Manaus-AM,
1056 Brazil, 40 pp., 2013.

1057 Trostdorf, C. R., Gatti, L. V., Yamazaki, a., Potosnak, M. J., Guenther, A., Martins, W. C. and Munger, J. W.:
1058 Seasonal cycles of isoprene concentrations in the Amazonian rainforest, Atmos. Chem. Phys. Discuss., 4(2),
1059 1291–1310, doi:10.5194/acpd-4-1291-2004, 2004.

1060 Unger, N., Harper, K., Zheng, Y., Kiang, N. Y., Aleinov, I., Arneth, a., Schurgers, G., Amelynck, C.,
1061 Goldstein, A., Guenther, A., Heinesch, B., Hewitt, C. N., Karl, T., Laffineur, Q., Langford, B., A. McKinney,
1062 K., Misztal, P., Potosnak, M., Rinne, J., Pressley, S., Schoon, N. and Serça, D.: Photosynthesis-dependent
1063 isoprene emission from leaf to planet in a global carbon-chemistry-climate model, Atmos. Chem. Phys.,
1064 13(20), 10243–10269, doi:10.5194/acp-13-10243-2013, 2013.

1065 Warneke, C., Gouw, J. A., Del Negro, L., Brioude, J., Mckeen, S., Stark, H., Kuster, W. C., Goldan, P. D.,
1066 Trainer, M., Fehsenfeld, F. C., Wiedinmyer, C., Guenther, A., B., Hansel, A., Wisthaler, A., Atlas, E.,
1067 Holloway, J. S., Ryerson, T. B., Peischl, j., Huey, L. G., Case Hanks, A. T.: Biogenic emission measurement
1068 and inventories determination of biogenic emissions in the eastern United States and Texas and comparison
1069 with biogenic emission inventories. J. Geophys. Res., 115(D00F18), doi:10.1029/2009JD012445, 2010.

1070 Yáñez-Serrano, A. M., Nölscher, A C., Williams, J., Wolff, S., Alves, E., Martins, G. a, Bourtsoukidis, E.,
1071 Brito, J., Jardine, K. J., Artaxo, P. and Kesselmeier, J.: Diel and seasonal changes of biogenic volatile organic
1072 compounds within and above an Amazonian rainforest, Atmos. Chem. Phys., 15, 3359–3378,
1073 doi:10.5194/acp-15-3359-2015, 2015.

1074 Zimmerman, P. R., Greenberg, J. P. and Westberg, C. E.: Measurements of atmospheric hydrocarbons and
1075 biogenic emission fluxes in the Amazon Boundary layer, J. Geophys. Res., 93(D2), 1407,
1076 doi:10.1029/JD093iD02p01407, 1988.

Table1: Isoprene and monoterpenes from different regions in the Amazonian rainforest: comparison of estimates and direct measurements of mixing ratios and fluxes.

Study	Site	Technical approach	isoprene (ppbv)	isoprene (mg m^{-2} h^{-1})	sum of Mt† (ppbv)	sum of Mt† (mg m^{-2} h^{-1})	season	comments
Central Amazonia								
Greenberg and Zimmerman, 1984	Manaus/Humaitá-Amazonas, Brazil	GC-FID, canister samples (near ground to 30m)	2.40 (1-5.24)[a]		2.86		Dry (Aug-Sep 1980)	mean - daytime range i not reported
Greenberg and Zimmerman, 1984	Manaus/Humaitá-Amazonas, Brazil	GC-FID, canister samples (flights from treetop to 2 km)	2.27 (0.38-4.08)[a]		5.47		Dry (Aug-Sep 1980)	mean - daytime range i not reported
Greenberg and Zimmerman, 1984	Manaus/Humaitá-Amazonas, Brazil	GC-FID canister samples (flights from 2km to Tropopause)	0.19 (0.14-0.22)[a]		1.91		Dry (Aug-Sep 1980)	mean - daytime range i not reported
Jacob and Wofsy, 1988*	ABLE - Adolfo Ducke Forest Reserve - Manaus-Amazonas, Brazil	Inverse modeling approach using Zimmerman et al. 1988 data		1.58			Dry (July-Aug 1985)	mean average of 24 hour
Zimmerman et al., 1988*	ABLE - Adolfo Ducke Forest Reserve - Manaus-Amazonas, Brazil	GC-FID, teflon bag on tethered balloon (30m)	2.65 [1.39-3.38] [b]		0.27 [0.15-0.54] [b]		Dry (July-Aug 1985)	median and interquartil range (24h)
Zimmerman et al., 1988*	ABLE - Adolfo Ducke Forest Reserve - Manaus-Amazonas, Brazil	GC-FID, teflon bag on tethered balloon (305m)	1.73 [1.03-2.15] [b]		0.15 [0.04-0.33] [b]		Dry (July-Aug 1985)	median and interquartil range (24h)
Zimmerman et al., 1988*	ABLE - Adolfo Ducke Forest Reserve - Manaus-Amazonas, Brazil	GC-FID, teflon bag on tethered balloon (up to 305m)		3.1		0.23	Dry (July-Aug 1985)	mean daytime (08:00 16:00, LT)
Rasmussen and Khalil, 1988	ABLE - Adolfo Ducke Forest Reserve - Manaus-Amazonas, Brazil	GC-FID, canister samples (near ground level)	2.77 (±0.4)				Dry (July-Aug 1985)	mean daytime (11:00 15:00, LT)
Rasmussen and Khalil, 1988	ABLE - Adolfo Ducke Forest Reserve - Manaus-Amazonas, Brazil	GC-FID, canister samples (aircraft flights from 150m to 5000m)	1.5 (±0.75)				Dry (July-Aug 1985)	daytime
Davis et al., 1994*	ABLE - Adolfo Ducke Forest Reserve - Manaus-Amazonas, Brazil	Mixed Layer Gradient approach using Zimmerman et al. 1988 data		3.63 (±1.4)			Dry (July-Aug 1985)	mean daytime (08:00 18:00, LT)
Kesselmeier et al., 2000	Balbina - ~100 km north of Manaus-Amazonas, Brazil	GC-MS, cartridge samples (outside forest)	6.55 (±1.26)		0.63 (±0.19)		Wet (Apr 1988)	mean daytime (09:30 15:00, LT)
		GC-MS, cartridge samples (inside Canopy)	3.55 (±0.07)		0.24 (±0.04)		Wet (Apr 1988)	mean daytime (09:30 15:00, LT)
		GC-MS, cartridge on tethered balloon (200-500m)	~3		~0.2		Wet (Apr 1988)	mean of 24h

Cont. **Table1:** Isoprene and monoterpenes from different regions in the Amazonian rainforest: comparison of estimates and direct measurements of mixing ratios and fluxes.

Study	Site	Technical approach	isoprene (ppbv)	isoprene (mg m^{-2} h^{-1})	sum of $Mt^{\dagger}$ (ppbv)	sum of $Mt^{\dagger}$ (mg m^{-2} h^{-1})	season	comments
Central Amazonia								
Kesselmeier et al., 2000	Cuieiras Biological Reserve (C14-ZF2) - Manaus-Amazonas, Brazil	GC-MS, cartridge samples (inside and above canopy)	6.7 ±1.07		0.73 ±0.24		Wet (Apr 1988)	daytime
Stefani et al. 2000	Cuieiras Biological Reserve (K34-ZF2) - Manaus-Amazonas, Brazil	GC-MS, cartridge on Relaxed Eddy Accumulation (~53m)		3.6 -5.4		0.72 – 0.9	Aug 1999 and Jan 2000	range of daytime averag normalized fluxes for th whole period of measurement
Andreae et al., 2002	Cuieiras Biological Reserve (K34-ZF2) - Manaus-Amazonas, Brazil	GC-MS, cartridge on Relaxed Eddy Accumulation (~53m)		2.88		0.36	Dry-Wet (Nov 1999-Jan 2000)	midday values
Ciccioli et al., 2003	Cuieiras Biological Reserve (K34-ZF2) - Manaus-Amazonas, Brazil	GC-MS, cartridge on Relaxed Eddy Accumulation (~51m)		5.11 max.		1.36 max.	Dry (July 2001)	midday values
Greenberg et al., 2004	Balbina - ~100 km north of Manaus-Amazonas, Brazil	GC-MS, cartridge on tethered balloon (200-1000m)	2.86 [2.25-3.64] [b]		0.21 [0.17-0.31] [b]		Wet (March 1998)	median and interquartiles daytime (12:00-15:00, LT)
Greenberg et al., 2004	Balbina - ~100 km north of Manaus-Amazonas, Brazil	Box model		5.3		0.23	Wet (March 1998)	maximum midday emissio fluxes estimated for th ecoregion
Karl et al., 2007††	Cuieiras Biological Reserve (C14-ZF2) - Manaus-Amazonas, Brazil	PTR-MS, Disjunct Eddy Covariance (~ 54 m)	7.8 ±3.7	8.3 ±3.1	0.87 ±0.3	1.7 ±1.3	Dry (Sep 2004)	mean daytime (12:00-14:00 LT)
Karl et al., 2007††	Cuieiras Biological Reserve (C14-ZF2) - Manaus-Amazonas, Brazil	PTR-MS, Mixed Layer Gradient (up to ~1200 m)	5.5 ±2.6	12.1 ±4.0	0.52 ±0.2	3.5 ±1.2	Dry (Sep 2004)	mean daytime (10:00-11:30 LT)
Kuhn et al., 2007**	Cuieiras Biological Reserve (K34-ZF2)- Manaus-Amazonas, Brazil	GC-FID, cartridge on Relaxed Eddy Accumulation (~51m)		2.4 ±1.8 (max. 6.1)		0.44 ±0.49 (max. 1.9)	Dry (July 2001)	mean daytime (10:00-15:00 LT)
Kuhn et al., 2007**	Cuieiras Biological Reserve (K34-ZF2) - Manaus-Amazonas, Brazil	GC-FID, cartridge on Surface Layer Gradient (28, 35.5, 42.5, 51m)		3.9 ±4.1 (max. 12.8)		0.43 ±0.65 (max. 2.1)	Dry (July 2001)	mean daytime (10:00-15:00 LT)
Kuhn et al., 2007**	Cuieiras Biological Reserve (K34-ZF2) - Manaus-Amazonas, Brazil	GC-FID, cartridge samples, Mixed Layer Gradient (50-3000m)		4.2 ±5.9 (max. 15.7)			Dry (July 2001)	mean daytime (10:00-18:00 LT)
Karl et al., 2009	Cuieiras Biological Reserve (TT34-ZF2) - Manaus-Amazonas, Brazil	PTR-MS, Gradient flux (2, 10.9, 16.7, 23.9, 30.3 and 39.8 m)		0.7 ±0.2			Wet (Feb 2008)	mean daytime (11:00-17:00 LT); flux at 35 m
Rizzo et al., 2010††	Cuieiras Biological Reserve (C14-ZF2)- Manaus-Amazonas,	PTR-MS, Disjunct Eddy Covariance (54 m)	7.8	8.4	0.29	0.93	Dry (Sep 2004) Dry (Sep 2004)	max. at early afternoon max. at noon

Cont. **Table1:** Isoprene and monoterpenes from different regions in the Amazonian rainforest: comparison of estimates and direct measurements of mixing ratios and fluxes.

Study	Site	Technical approach	isoprene (ppbv)	isoprene (mg m^{-2} h^{-1})	sum of Mt† (ppbv)	sum of Mt† (mg m^{-2} h^{-1})	season	comments
Central Amazonia								
Silva, 2010	Cuieiras Biological Reserve (K34-ZF2)- Manaus-Amazonas, Brazil	GC-MSFID cartridge samples at 1m	3.2 ±0.9		0.28 ±0.13		Wet (May 2009)	mean daytime (07:00-17:00 LT)
		GC-MSFID cartridge samples at 10m	4.6 ±0.94		1.09 ±0.35		Wet (May 2009)	mean daytime (07:00-17:00 LT)
		GC-MSFID cartridge samples at 20m	6.17 ±1.03		0.75 ±0.17		Wet (May 2009)	mean daytime (07:00-17:00 LT)
Tardine et al., 2011‡	Cuieiras Biological Reserve (TT34-ZF2)- Manaus-Amazonas, Brazil	PTR-MS, Gradient profile (2, 11, 17, 24, 30 and 40 m)			~ 0.78		Dry-Wet (Sep-Dec 2010)	mean daytime 10:00-16:00 LT) at 40 m
Tardine et al., 2011‡	Cuieiras Biological Reserve (TT34-ZF2)- Manaus-Amazonas, Brazil	PTR-MS, Gradient profile (2, 11, 17, 24, 30 and 40 m)				~ 1.47	Dry-Wet (Sep-Dec 2010)	mean daytime 10:00-16:00 LT) at 35 m
Tardine et al., 2012‡	Cuieiras Biological Reserve (TT34-ZF2)- Manaus-Amazonas, Brazil	PTR-MS, Gradient profile (2, 11, 17, 24, 30 and 40 m) and Gradient flux		~1.43			Dry-Wet (Sep-Dec 2010)	mean daytime (10:00-16:00 LT); flux at 40 m
Yáñez-Serrano et al., 2015	ATTO site - Manaus Manaus-Amazonas, Brazil	PTR-MS, Gradient profile (0.05, 0.5, 4, 24, 38, 53 and 79 m)	5.22 ±1.5		0.75 ±0.18		Dry (Sep 2013)	Isoprene, daytime median (12 15:00, LT). Mt, daytime median (15-18:00, LT)
Yáñez-Serrano et al., 2015	ATTO site - Manaus Manaus-Amazonas, Brazil		1.5 ±0.78		< 0.23		Wet (Feb-Mar 2013)	Isoprene, daytime median (12 15:00, LT). Mt, daytime median (15-18:00, LT)
This study‡	Cuieiras Biological Reserve (TT34-ZF2) - Manaus-Amazonas, Brazil	PTR-MS, Gradient profile (2, 11, 17, 24, 30 and 40 m) and Gradient flux	2.68 ±0.9	1.37 ±0.7	0.67 ±0.3	1.47 ±0.06	Dry (Sep-Oct 2010)	mean daytime (10:00-14:00, LT) at 40m
This study‡	Cuieiras Biological Reserve (TT34-ZF2) - Manaus-Amazonas, Brazil	PTR-MS, Gradient profile (2, 11, 17, 24, 30 and 40 m) and Gradient flux	2.65 ±1.33	1.41 ±0.1	0.85 ±0.4	1.29 ±0.2	DWT¥ (Nov 2010)	mean daytime (10:00-14:00, LT) at 40m
This study‡	Cuieiras Biological Reserve (TT34-ZF2) - Manaus-Amazonas, Brazil	PTR-MS, Gradient profile (2, 11, 17, 24, 30 and 40 m) and Gradient flux	1.66 ±0.9	0.52 ±0.1	0.47 ±0.2	0.36 ±0.05	Wet (Dec 2010 -Jan 2011)	mean daytime (10:00-14:00, LT) at 40m
Eastern central Amazonia								
Rinne et al., 2002	Tapajós National Forest - Santarém-Pará, Brazil	GC-MS cartridge on Disjunct Eddy Accumulation (~ 45m)	5 max.	2.4			Dry (July 2000)	Afternoon values 30 ºC and 1000 µmol m^{-2} s^{-1}
Greenberg et al., 2004	Tapajós National Forest - Santarém-Pará, Brazil	GC-MS, cartridge on tethered balloon (200-1000m)	0.74 [0.6-1] [b]		0.08 [0.03-0.06] [b]		Wet (Jan-Feb 2000)	median and interquartiles daytime (12:00-15:00, LT)
Greenberg et al., 2004	Tapajós National Forest - Santarém-Pará, Brazil	Box model		2.2		0.18	Wet (Jan-Feb 2000)	maximum midday emissio fluxes estimated for th ecoregion

Cont. **Table1:** Isoprene and monoterpenes from different regions in the Amazonian rainforest: comparison of estimates and direct measurements of mixing ratios and fluxes.

Study	Site	Technical approach	isoprene (ppbv)	isoprene (mg m^{-2} h^{-1})	sum of Mt[†] (ppbv)	sum of Mt[†] (mg m^{-2} h^{-1})	season	comments
Eastern central Amazonia								
Trostdorf et al., 2004	Tapajós National Forest - Santarém-Pará, Brazil	GC-FID, canister samples (54, 64 m)	1.9 ±1.2; 1.3 ±0.8				Wet (Jan- May 2002)	mean daytime (11:00-14:00 LT)
Trostdorf et al., 2004	Tapajós National Forest - Santarém-Pará, Brazil	GC-FID, canister samples (54, 64 m)	1.4 ±0.5; 1.0 ±0.4				WDT[¥¥] (June-July 2002)	mean daytime (11:00-14:00 LT)
Trostdorf et al., 2004	Tapajós National Forest - Santarém-Pará, Brazil	GC-FID, canister samples (54, 64 m)	2.8 ±0.9; 2.5 ±0.8				Dry (Aug-Nov 2002)	mean daytime (11:00-14:00 LT)
Western Amazonia								
Helmig et al., 1998	Peru - 500 km west of Iquitos	GC-MS, cartridge on tethered balloon (up to 1600 m)	3.31, 1.39, 0.16		0.21, 0.06, 0.015		July 1996	Median daytime (ground mixed layer and above mixed layer)
Helmig et al., 1998	Peru - 500 km west of Iquitos	GC-MS, cartridge samples, Mixed Layer Gradient		7.4		0.42		mean daytime
Helmig et al., 1998	Peru - 500 km west of Iquitos	GC-MS, cartridge samples, Mixed Layer Budget		8.1		0.41		mean daytime
Southern Amazonia								
Kesselmeier et al., 2002	Jaru Biological Reserve, Rondônia, Brazil	GC-FID, cartridge samples (8-52m)	~4		~0.8		WDT[¥¥] (May 1999)	mean daytime (11:00-18:00 LT)
Kesselmeier et al., 2002	Jaru Biological Reserve, Rondônia, Brazil	GC-FID, cartridge samples (8-52m)	~12		~0.8		DWT[¥] (Sep-Out 1999)	mean daytime (11:00-18:00 LT)
Greenberg et al., 2004	Jaru Biological Reserve, Jaru-Rondônia, Brazil	GC-MS, cartridge on tethered balloon (200-1000m)	6.89 [2.78-7.73] [b]		0.83 [0.56-2.65] [b]		Wet (Feb 1999)	median and interquartiles daytime (12:00-15:00, LT)
Greenberg et al., 2004	Jaru Biological Reserve, Jaru-Rondônia, Brazil	Box model		9.8		6.1	Wet (Feb 1999)	maximum midday emissio fluxes estimated for th ecoregion
Simon et al., 2005	Jaru Biological Reserve, Rondônia, Brazil	Lagrangian transport sub-model.		~5.9			WDT[¥¥] (May 1999)	midday values
Simon et al., 2005	Jaru Biological Reserve, Rondônia, Brazil	Modeling using data of Kesselmeier et al., 2002		~8.2			DWT[¥] (Sep-Out 1999)	midday values

Cont. **Table1:** Isoprene and monoterpenes from different regions in the Amazonian rainforest: comparison of estimates and direct measurements of mixing ratios and fluxes.

Study	Site	Technical approach	isoprene (ppbv)	isoprene (mg m^{-2} h^{-1})	sum of Mt† (ppbv)	sum of Mt† (mg m^{-2} h^{-1})	season	comments
Southern Amazonia								
Aquino, 2006	Jaru Biological Reserve, Rondônia, Brazil	GC-FID, canister samples (50, 60 m)	4.5 ±0.9; 4.0 ±1.2				Wet (Feb-May 2002)	mean daytime (11:00-16:00 LT)
Aquino, 2006	Jaru Biological Reserve, Rondônia, Brazil	GC-FID, canister samples (50, 60 m)	2.1 ±2.0; 1.8 ±1.8				WDT¥¥ (Jun 2002)	mean daytime (11:00-16:00 LT)
Aquino, 2006	Jaru Biological Reserve, Rondônia, Brazil	GC-FID, canister samples (50, 60 m)	4.6 ±2.7; 4.0 ±2.5				Dry (Jul-Sep 2002)	mean daytime (11:00-16:00 LT)
Aquino, 2006	Jaru Biological Reserve, Rondônia, Brazil	GC-FID, canister samples (50, 60 m)	3.4 ±1.2; 3.0 ±0.5				DWT¥ (Out-Nov 2002)	mean daytime (11:00-16:00 LT)

Note: Seasons follow determination of each study. For some studies the exact times of sample collection are not available and then not reported. Statistics differed among studies. The most of studies showed mean values but others presented median values and/or just a range of all values measured.

†Mt - monoterpenes;

[a]- range of variation;

[b] - interquartile ranges based on median "[]";

*, ** studies derived from the same observational data base;

‡, †† studies derived from part of the same observational data base;

¥DWT - dry-to-wet transition season;

¥¥WDT - wet-to-dry transition season.

Figures

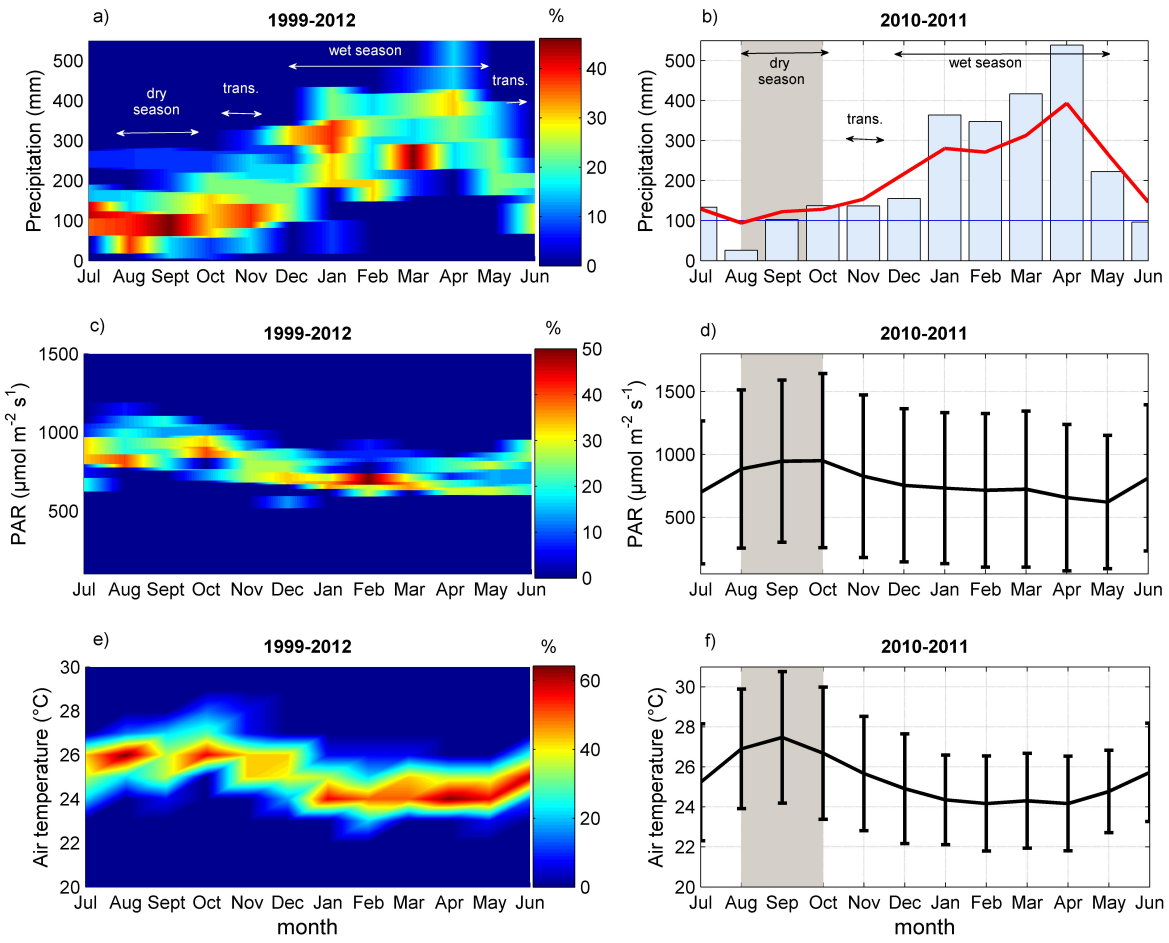

Figure 1: Precipitation, PAR and air temperature measured at K34 tower (~2 km far of TT34 tower); a) relative frequency (%) of monthly cumulative precipitation from 1999 to 2012, b) monthly cumulative precipitation from July 2010 to June 2011 (measured in 30 minute intervals for 24 hours) (bars), and average of monthly cumulative precipitation from 1999 to 2012 (red line); c) relative frequency of monthly PAR from 1999 to 2012 (measured every 30 min during 06:00-18:00, LT), d) monthly average PAR from July 2010 to June 2011 (measured every 30 min during 06:00-18:00, LT); e) relative frequency of monthly air temperature from 1999 to 2012, f) monthly average air temperature from July 2010 to June 2011 (measured in 30 minute intervals for 24 hours). Figures on the right side cover the period of this study; grey areas represent the period of dry season; and blue line at (b) represents 100 mm month^{-1}. Error bars represent one standard deviation.

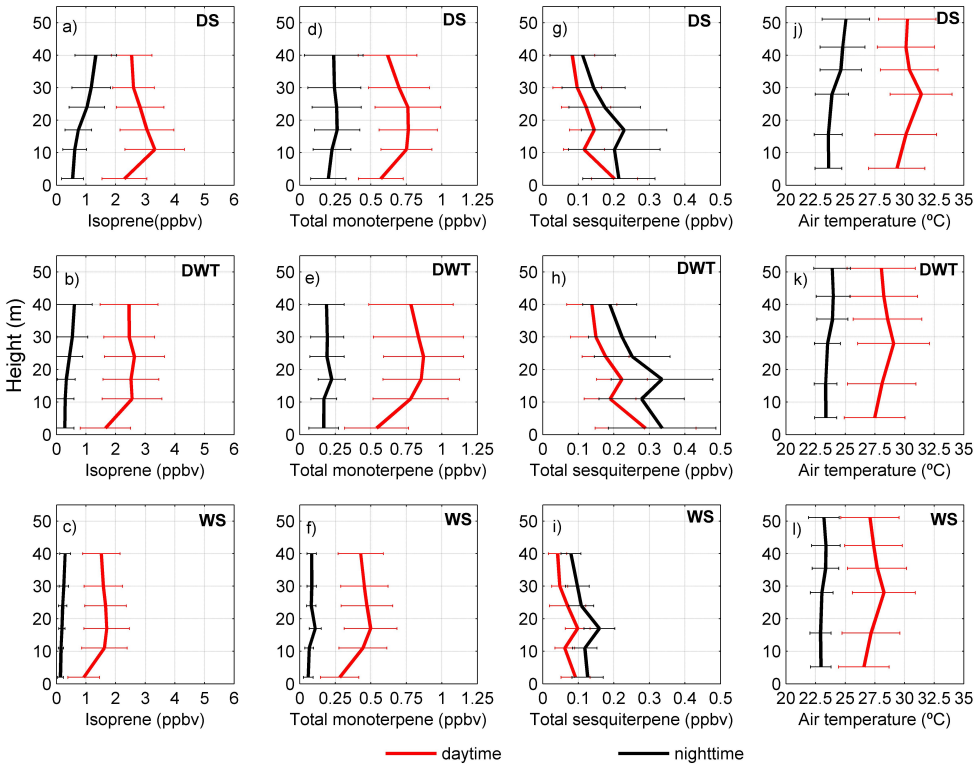

Figure 2: Daytime (10:00-16:00, LT) and nighttime (22:00-04:00, LT) average vertical profiles of isoprene (a, b, c), total monoterpenes (d, e, f), total sesquiterpenes (g, h, i), and air temperature (j, k, l) of the dry season (DS), the dry-to-wet transition season (DWT) and the wet season (WS). Error bars represent one standard deviation.

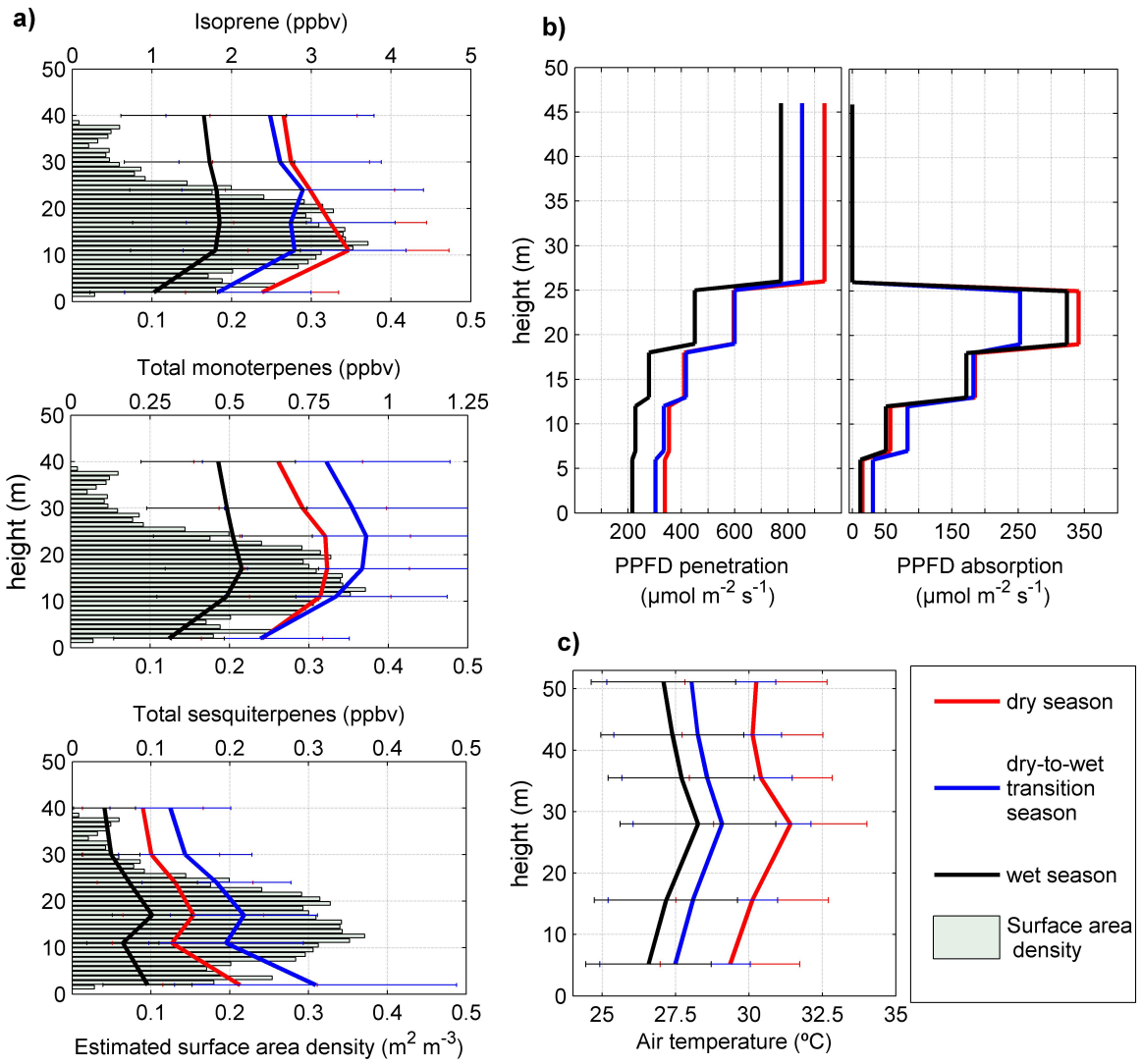

Figure 3: Daytime (10:00-16:00, LT) vertical profiles of mixing ratios of isoprene, total monoterpenes and total sesquiterpenes from the dry season to the wet season; and estimated surface area density of the canopy at this study site (ground-based measurements carried out in March/2004 using LIDAR - Light Detection And Ranging) (Parker and Fitzjarrald, 2004) (a). Vertical profile of photosynthetic photon flux density (PPFD) penetration and absorption by the canopy from the dry season to the wet season modeled by MEGAN 2.1 (b). Daytime (10:00-16:00, LT) air temperature profiles from dry season to wet season measured at K34 tower (c). In fig. 1a the top and the bottom x axis represent isoprenoid mixing ratios and estimated surface area density of the canopy, respectively. Error bars represent one standard deviation.

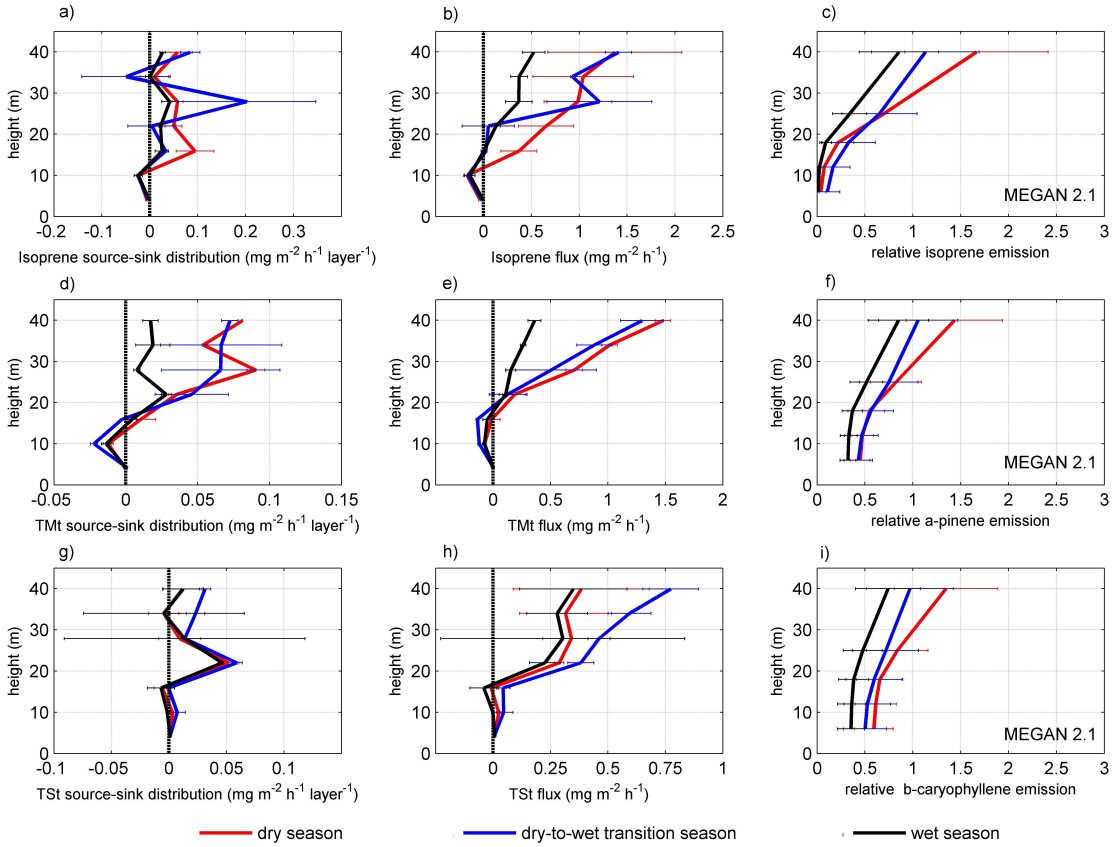

Figure 4: Daytime (10:00-14:00, LT) source-sink distribution inside and above the canopy, cumulative flux estimation, and relative emission modeled by MEGAN 2.1 of isoprene (a, b, c), total monoterpenes (TMt) (d, e, f) and total sesquiterpenes (TSt) (g, h, i) from the dry season to the wet season. Error bars represent one standard deviation.

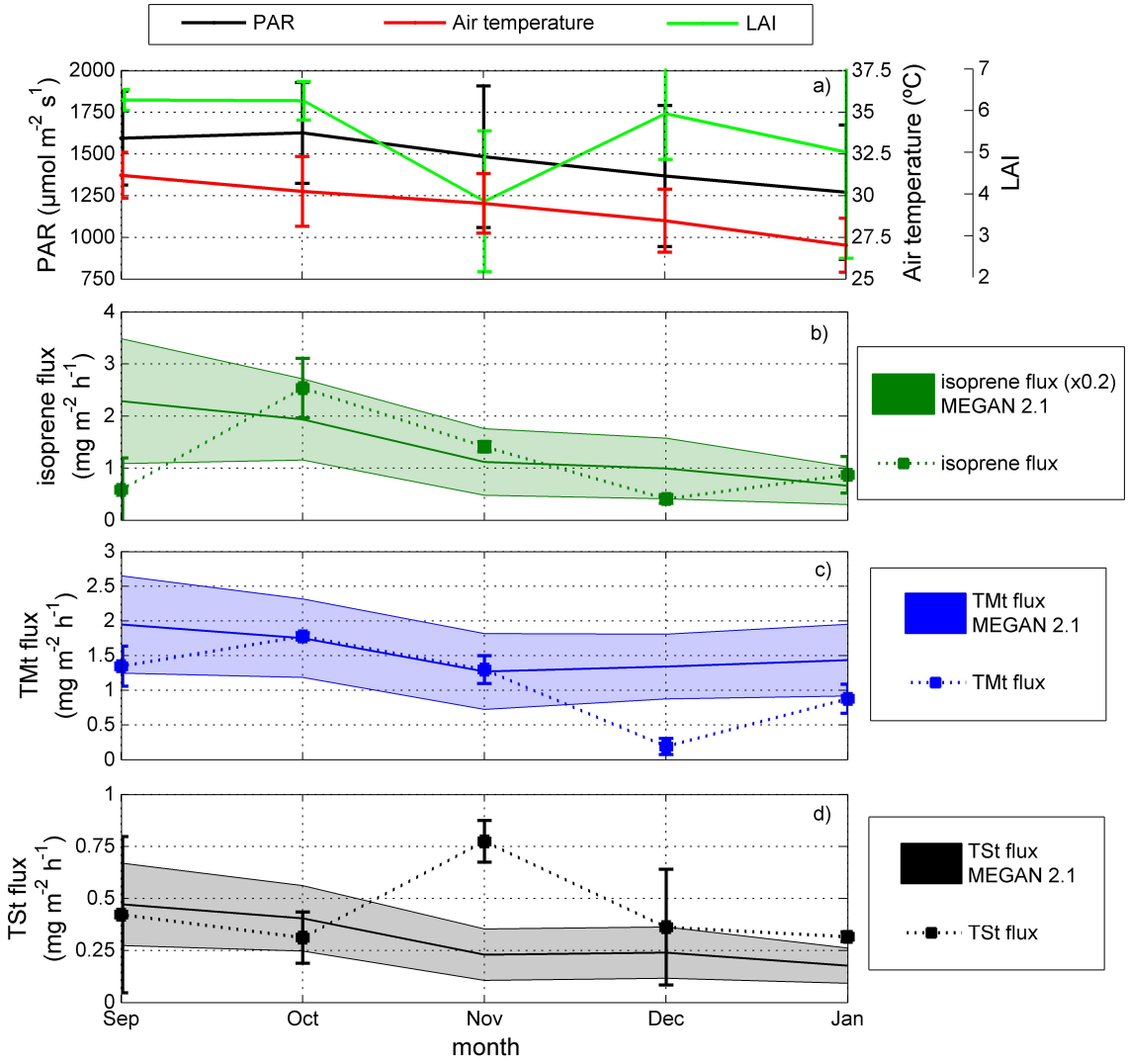

Figure 5: Monthly averages of air temperature and PAR (measured at K34 tower during 10:00-14:00, LT), and LAI (MODIS, 8-day observations) (a). Monthly averages of fluxes of isoprene (b), total monoterpenes (TMt) (c) and total sesquiterpenes (TSt) (d). Flux based on in-situ PTR-MS measurements (inverse Lagrangian transport model - estimates for 10:00-14:00, LT, at TT34 tower) are represented by solid squares and one standard deviation; fluxes modeled by MEGAN 2.1 (estimates for 10:00-14:00, LT) are shown by solid lines and filled areas that represent one standard deviation. Isoprene flux modeled by MEGAN 2.1 in (b) were divided by five. Error bars represent one standard deviation.

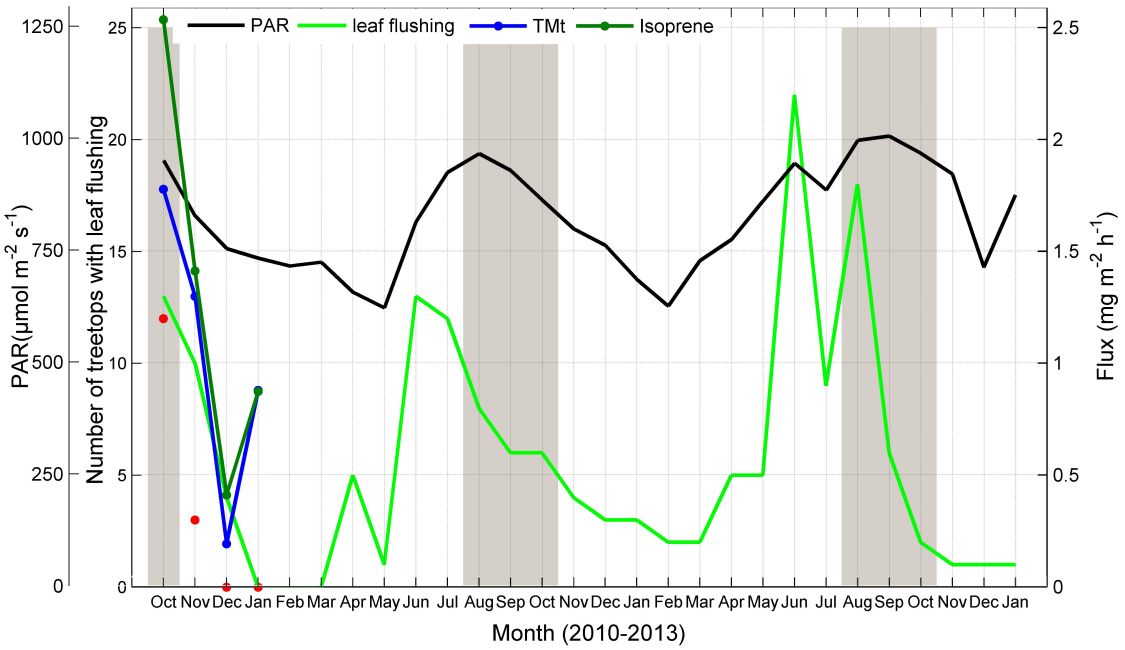

Figure 6: Estimated monthly leaf flushing (light green line) (Tavares, 2013), and monthly average of PAR measured from October 2010 to January 2013 at K34 tower (06:00-18:00, LT) (black line). For the period of this study, leaf flushing is also represented by the analysis of canopy images for every six days from October 2010 to January 2011 (red circles). Monthly averages of fluxes of isoprene (dark green line) and total monoterpenes (blue line) (estimated for 10:00-14:00, LT, at TT34 tower). Grey areas represent the period of the dry season.

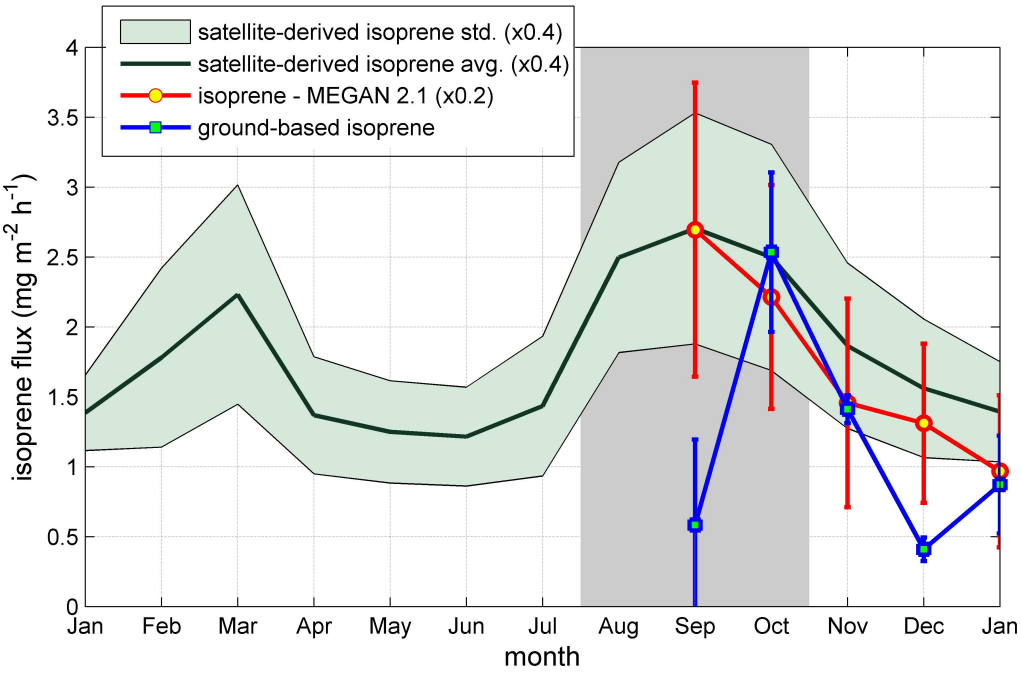

Figure 7: Comparison of monthly isoprene emissions based on in-situ PTR-MS measurements (inverse Lagrangian transport model) and satellite-derived estimates and MEGAN 2.1 estimates. Satellite-derived estimates are from January 2010 to January 2011, and ground-based estimates are from September 2010 to January 2011. Satellite-derived and MEGAN 2.1 estimates were divided by 2.5 and 5, respectively. Grey area represents the period of the dry season. Error bars represent one standard deviation.